AD-A124 677 AN EXPERIMENTAL STUDY OF CLUSTER NOZZLE PERFORMANCE(U) 1/1
AIR FORCE INST OF TECH WRIGHT-PATTERSON AFB OH SCHOOL
OF ENGINEERING J T LESTER DEC 82 AFIT/GAE/AA/82D-18
UNCLASSIFIED F/G 21/8 NL

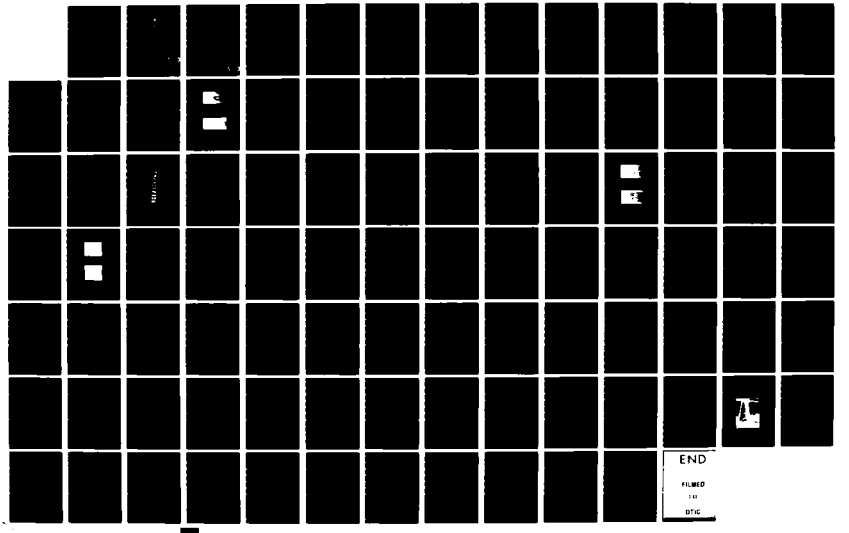

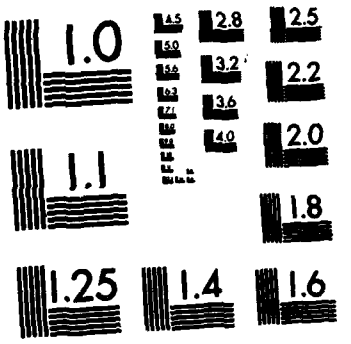

AN EXPERIMENTAL STUDY OF CLUSTER NOZZLE PERFORMANCE

THESIS

AFIT/GAE/AA/82D-18 James T. Lester, Jr.
Capt. USAF

DEPARTMENT OF THE AIR FORCE
AIR UNIVERSITY (ATC)
AIR FORCE INSTITUTE OF TECHNOLOGY

Wright-Patterson Air Force Base, Ohio

AFIT/GAE/AA/82D-18

AN EXPERIMENTAL STUDY
OF
CLUSTER NOZZLE PERFORMANCE

THESIS

AFIT/GAE/AA/82D-18 James T. Lester, Jr.
Capt. USAF

AFIT/GAE/AA/82D-18

AN EXPERIMENTAL STUDY
OF
CLUSTER NOZZLE PERFORMANCE

THESIS

Presented to the Faculty of the School of Engineering
of the Air Force Institute of Technology
in Partial Fulfillment of the
Requirements for the Degree of
Master of Science

By
James T. Lester, Jr., B.S.
Capt. USAF

Graduate Aeronautics and Astronautics

December 1982

Acknowledgments

By working on this thesis, I have learned the two most important requirements for the successful completion of a research project. Hard work is the first requirement, and that is solely dependent on the person doing the research. The second requirement is strong support. I would like to take time now to acknowledge some of the support I received during this study.

My thesis advisor, Dr. W. C. Elrod, was an immense source of experience to draw upon, and his interest in me both as a student and person is deeply appreciated. My thesis committee, Maj. E. Jumper and Capt. W. Cox, contributed in their individual ways to enhance the quality of this thesis. Dr. P. Torvik's help with the visicorder is also appreciated.

The lab technicians, Mr. Baker and Mr. Cannon, provided much needed support throughout the study. The support of the A.F.I.T. fabrication shop, especially Mr. Shortt and Mr. Brohas, was excellent and contributed significantly to the completion of this work. A thank you goes to Mrs. D. Docken for the typing of this thesis.

Capt. R. Moore, a personal friend and classmate, has me forever in his debt. Not only was he there on a daily basis to provide a third hand, he also provided the means to do my many plots by computer.

Finally, I would like to thank my wife, Stephanie, for her patience and love during this time at A.F.I.T. Unfortu-

nately, she has only been married to an A.F.I.T. student and deserves so much better. May God continue to bless her.

James T. Lester, Jr.

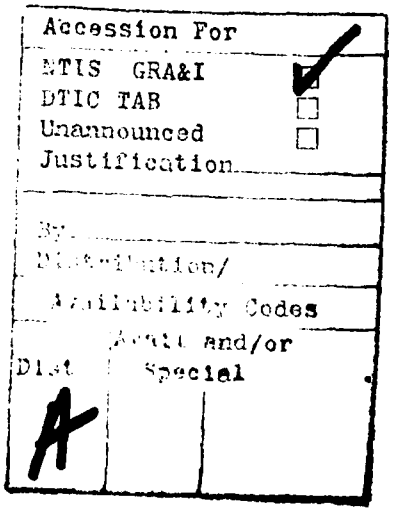

Contents

List of Figures

Figures Page

Figures Page

List of Tables

List of Symbols

a	speed of sound (f/s)
A_e	nozzle exit area (in^2)
A_t	nozzle throat area (in^2)
C_1	combined mass flow constant
C_f	thrust coefficient
C_{f_c}	thrust coefficient calculated from mass flow
C_{f_m}	measured thrust coefficient
C_{f_t}	theoretical thrust coefficient
d	diameter of orifice (in)
g_c	= 32.17 $(lbm \cdot f)/(lb_f \cdot s^2)$
K	flow constant
L	divergent length of nozzle (in)
M_e	exit Mach number
M_t	throat Mach number
m	mass flow rate (lbm/s)
P_a	pressure prior to orifice (psi)
P_e	exit pressure (psi)
P_o	chamber pressure (psi)
P_3	ambient pressure (psi)
PR	pressure ratio
R	nozzle throat radius (in)
R_c	gas constant $(lb_f \cdot f/R \cdot lbm)$
r	nozzle exit plane radius (in)
T	thrust (lb_f)
t_a	temperature prior to orifice (R)
t_e	exit temperature (R)

t_o	chamber temperature (R)
t_t	throat temperature (R)
V_e	exit gas velocity (f/s)
V_t	throat gas velocity (f/s)
Z	compressibility factor
γ	ratio of specific heats (=1.4)
ρ	air density (lbm/f^3)
ρ_t	throat density (lbm/f^3)

Abstract

Clusters of up to ten converging-diverging supersonic nozzles were cold flow tested at ambient conditions to determine their thrust performance as compared to a single nozzle of the same total throat area. The nozzles were operated at both underexpanded and overexpanded conditions, and no significant thrust difference was detected between the clusters and single nozzles. Schlieren photographs verified no interference between the jets of different nozzles. Clusters with various patterns of flowing and non-flowing nozzles were also tested. The non-flowing nozzles had no effect on the flowing nozzles except when, due to the sealed nozzles, the base plate area was greatly increased. The increased base plate area resulted in a noticeable improvement of thrust over theoretical throughout the pressure ratio range tested with the greatest increase in the underexpanded region. The locations or patterns of non-flowing nozzles were of no consequence. Finally, aerodynamic shrouding, with no spacing between the shrouding and the nozzle, was placed on the clusters and tested. There was a very slight decrease in thrust performance associated with a decrease in the base plate effect.

I Introduction

The Air Force Rocket Propulsion Laboratory (AFRPL), Edwards A.F.B., California, is looking into the possibility of using clustered R1-10 rocket engines to power single stage orbital vehicles. They hope to obtain better performance out of a multi-nozzle assembly than a single large nozzle engine. The expected increase in performance should not only be due to better specific impulse but also due to better aerodynamic characteristics in the atmospheric portion of the flight.

Background

A rocket engine nozzle acts to accelerate or expand the combustion gases to a very high velocity, which with the mass flow creates the desired thrust. The amount the gases are expanded is determined by the physical geometry of the nozzle, but due to various chamber pressures, the pressure at the exit of the nozzle can vary. The total thrust of an engine is not only a function of the exit velocity of the gases, but also the difference between the exit gas pressure and the ambient pressure. For a single nozzle conservation of momentum gives:

$$T = \frac{\dot{m} V_e}{g_c} + (P_e - P_3)\, A_e \qquad (1)$$

where

T = thrust (lb_f)
$\dot{m}$ = mass flow (lbm/s)
V_e = exit velocity (f/s)

P_e = exit pressure (psi)
P_3 = ambient pressure (psi)
A_e = exit area (in^2)
g_c = conversion factor
= 32.2 $(lbm \cdot f)/(lb_f \cdot s^2)$

If the exit pressure is lower than the ambient pressure, a negative pressure thrust results. This operating condition is referred to as overexpansion. Overexpansion causes the exhaust jet to contract. Fig. 1a shows the resulting contraction, along with the oblique shock waves required to increase the exhaust pressure to ambient pressure.

If the exit and ambient pressures are equal, then the nozzle is perfectly expanded. This is the optimal flow condition and there is no contraction or oblique shocks in the plume.

The final case is when the exit pressure is greater than the ambient pressure and this is called underexpansion. The pressure thrust is a positive value, but the velocity term is not at its maximum, and, therefore, the thrust is not at its optimal value. The exhaust jet expands outwards as shown in Fig. 1b. The expansion waves required to reduce the pressure to ambient conditions are also present.

For this study, the effect of nozzle jet shape is of significance due to the potential of one jet from a nozzle interfering with a jet from another nozzle in a cluster as reported by Goethert (Ref. 3). The interaction of two or more jets will affect the performance of the cluster as a whole.

The interaction effect was first noticed on the Polaris missile (Ref. 2), which used a four-nozzle cluster. At high altitudes, a noticeable thrust augmentation would

a) Overexpanded Flow
(PR = 11)

b) Underexpanded Flow
(PR = 25)

Figure 1. Schlieren Photographs of Flow from a Single Nozzle (Nozzle 03)

occur. Goethert (Ref. 3) studied the Polaris case in detail and concluded that at high altitudes (greater than 60,000 feet), the four jets would intersect due to underexpansion. The intersection would cause a pressure build up in the area between the nozzles which exerted a force on the base area of the rocket. The jets would act as walls preventing the pressure from escaping. The thrust augmentation of .3 to .4 percent was measured. Unfortunately, Goethert limited his study to just the Polaris configuration. Harper (Ref. 4) confirmed Goethert's work with the Black Knight rocket of similar configuration. Harper also looked into the increased heating problems of the base area due to the pressure rise. Rudov (Ref. 7) used shadow photographs to examine the flow contours of two-nozzle and four-nozzle configurations. In this work, he did not directly address any performance changes due to the flow conditions.

Hibson (Ref. 5) studied the performance characteristics of two-nozzle, four-nozzle and six-nozzle configurations at sea level. His configurations were very similar to what the AFRPL was proposing to use for single stage orbital vehicles. His results, at the pressures tested, were that the two-nozzle configuration performed slightly better than the rest. The results were only preliminary, and more research is required.

Objectives

As a continuation of Hibson's work, this study had two main objectives:

1. To experimentally determine the effect of non-flowing nozzles on the performance of the rest of the nozzles in a cluster. Special emphasis was placed on the effects due to patterns and locations of non-flowing nozzles.

2. To experimentally determine the effect of an aerodynamic shroud on the performance of a multi-nozzle cluster.

Approach

Cold flow scale model testing using compressed air was done to meet this study's particular objectives. Though the thrust was the main parameter measured, the thrust coefficient was used to compare different configurations. The thrust coefficient is defined by:

$$C_f = T/P_O A_t \qquad (2)$$

where

C_f = thrust coefficient
T = thrust (lb_f)
P_O = chamber or tank pressure (psi)
A_t - throat area (in^2)

The thrust coefficient allows a comparison of configurations of different throat areas. The throat area used was the total throat area of the flowing nozzles in a configuration. For a more direct comparison, the multi-nozzle configurations were compared to single nozzle of the same total throat area. The performance of each nozzle was also compared to the theoretical value of thrust coefficient. The theoretical thrust coefficient is based on isentropic flow and ignores viscous or base pressure effects. The theoretical value is given by (Ref. 8):

$$C_{f_t} = \sqrt{\frac{2\gamma^2}{\gamma-1}\left(\frac{2}{\gamma+1}\right)^{(\gamma+1)/(\gamma-1)}\left[1-\frac{Pe}{Po}^{\frac{\gamma-1}{\gamma}}\right]} + \frac{(Pe-P_3)}{Po}\frac{Ae}{At} \qquad (3)$$

where

C_{f_t} = theoretical thrust coefficient
γ = ratio of specific heats
= 1.4

The viscous effects can be determined by comparing the actual data with the theoretical values calculated by the above equation.

II Experimental Apparatus

In order to compare thrust coefficients of various nozzle configurations, the thrust must be measured as accurately as possible. The stilling chamber and gas supply system was designed as a pendulum type assembly to permit accurate thrust measurement. An overall schematic is given in Fig. 2, and an overall photograph is given in Fig. B-1. The thrust was measured directly by the use of a strain gauge mounted on a cantilever beam, but thrust also can be calculated using the mass flow and the tank conditions (pressure and temperature). The apparatus included the necessary instrumentation for temperature and pressure measurement that made the indirect calculation possible. The calculation method does not account for any thrust changes due to interactions outside the nozzle due to choke flow condition.

Table I lists the main instrumentation equipment used in this study. The experimental apparatus has four parts: the flow system, the thrust measuring system, the flow instrumentation and the test articles. The test articles are the single and clustered nozzles necessary for the study.

Flow System

The flow medium was compressed air supplied by a gas trailer containing 36 interconnectable cylinders which could be filled to 2,300 psig. The flow system is shown schematically in Fig. 3. A Grove regulator in combination with a dome

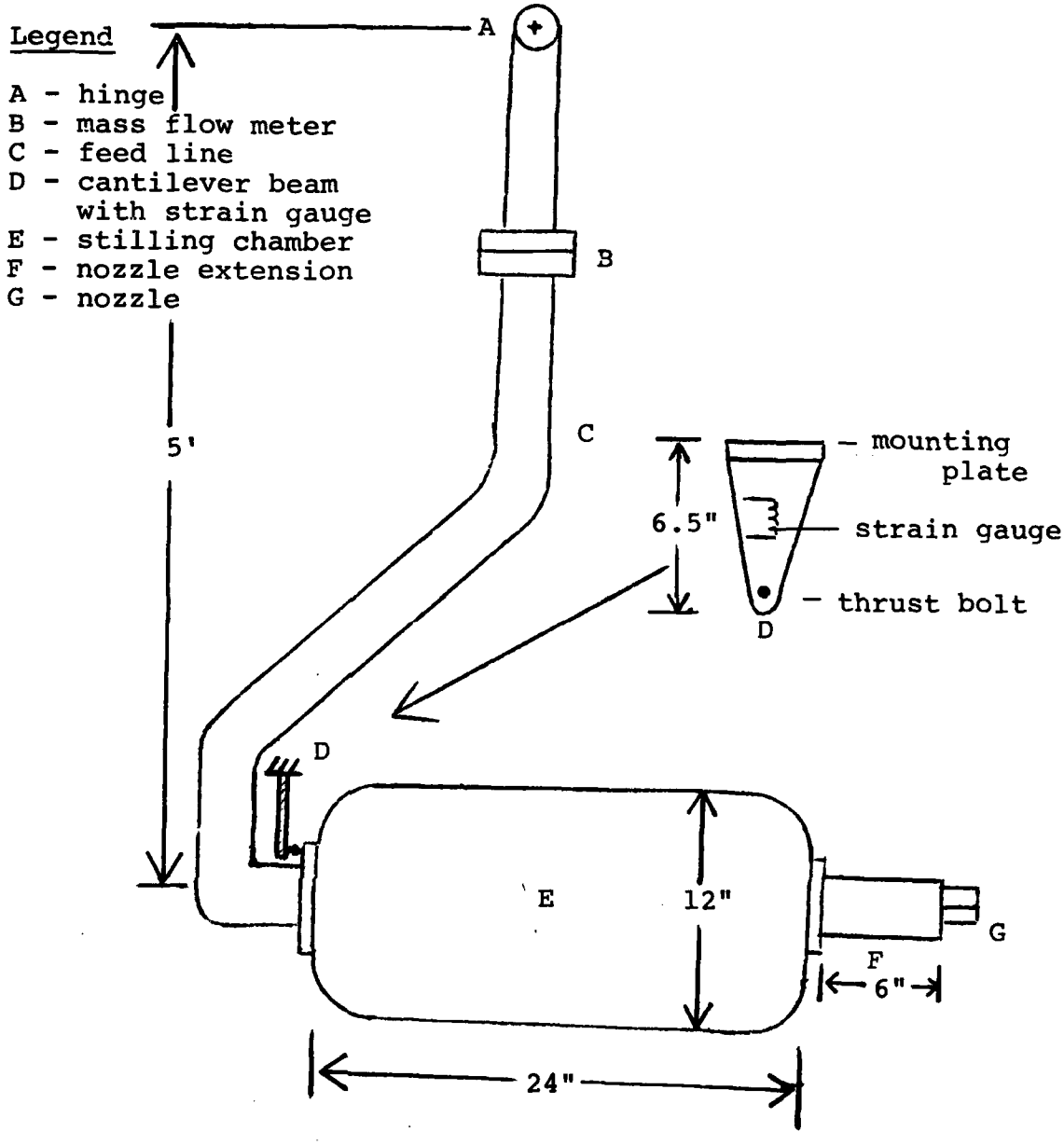

Figure 2. Thrust Measurement System

Table I Test Equipment

Item	Model No.	Serial No.
Grove Regulator	15-L	L34138
Dome Regulator	WBX205-K3	105040-7
Power Supply (Hewlett-Packard)	6205B	1949A1664
Power Supply (Hewlett-Packard)	6205B	1949A1665
Pressure Transducer (Statham)	206 (0-500 psig)	662567
Pressure Transducer (Statham)	206 (0-500 psig)	662568
Pressure Transducer (Statham)	2301 (0-1000 psig)	0671553
Pressure Transducer (Statham)	551 (± 5 PSID)	PM280TC±5-350
Visicorder (Honeywell)	1508	15-2882
Mass Flow Meter	Orifice	
Load Cell	Strain Gauge Bridge	
Thermocouple	Cu/Const.	

regulator, was used to adjust the pressure from 150 psig to 350 psig in the stilling tank. A stilling chamber was used to provide a uniform, well defined condition at the inlet to the nozzle assembly. The flow was passed through a perforated cylinder to minimize the size and weight of the hinged flow assembly. An extension was used on the tank to eliminate any base pressure effect due to the close proximity of the tank to the nozzle exit plane. The nozzles were attached to the end of the extension, which was big enough to provide a negligible approach velocity on the nozzle inlet. An oval extension was used for the bigger clusters, while a smaller round extension was used for the single nozzles and smaller clusters. An o-ring made the connection air tight. The tank had a single tap for both pressure and temperature measurements.

Thrust Measuring System

The stilling chamber was on a five-foot arm that could rotate about a hinge point. To provide a smooth transition at the hinge point, the flow passed through slots in the horizontal pipe to go into the vertical pipe. Design details are presented in Ref. 5. O-ring seals were used to seal the hinge point. At the bottom of the hinge arm, the chamber rested against a round headed bolt attached to an aluminum cantilever beam located at the opposite end of the chamber from the nozzles. See Fig. 2 for details. When a thrust was applied, the pendulum assembly was free to rotate about the hinge point causing the force to be applied to the bolt, which in turn would cause the aluminum beam to bend slightly.

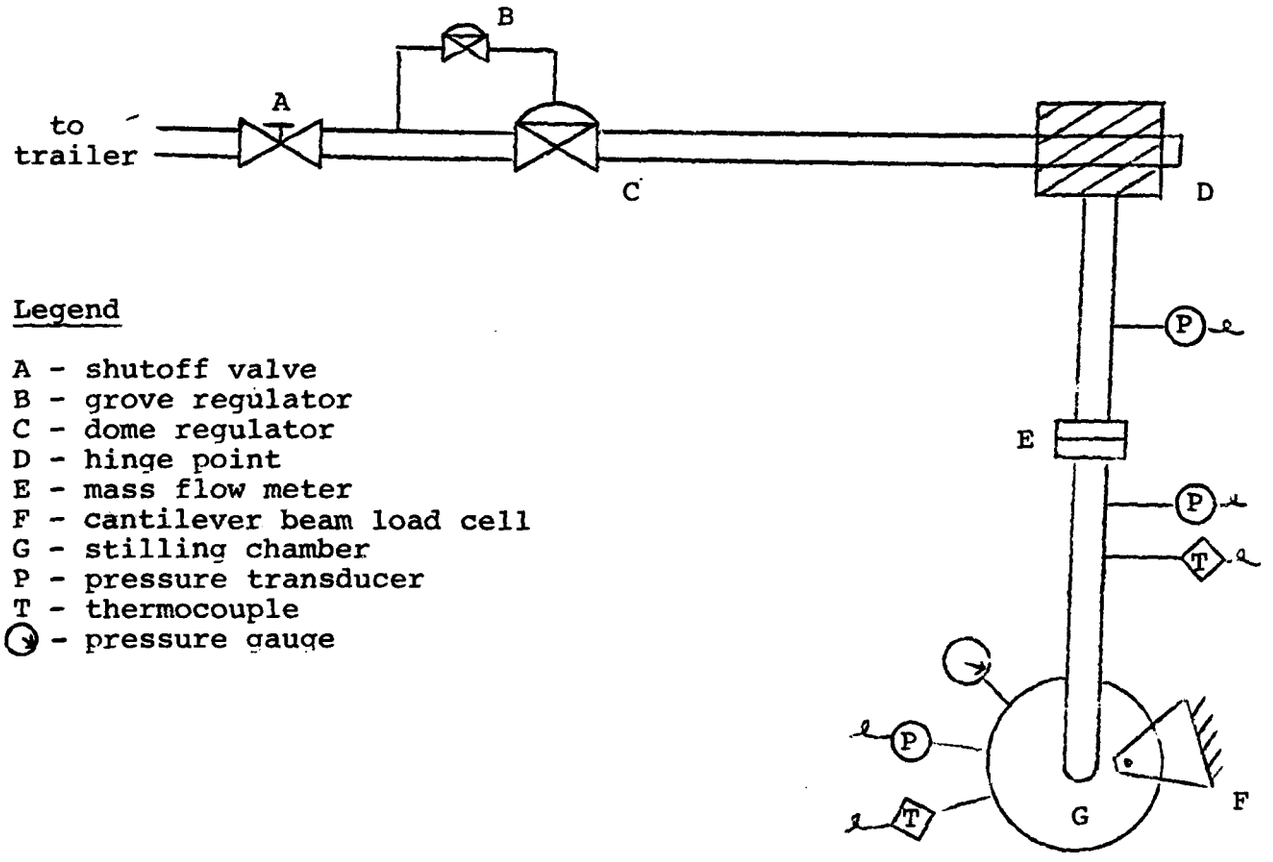

Figure 3. Flow System Schematic

A strain gauge mounted on the beam converted the bending to an electrical signal proportional to the applied force. The rotation was small enough that the force still acted in a horizontal direction. Though the movement at the hinge point was very small, any binding due to friction would cause erroneous thrust measurements. To help alleviate this problem, bearings were installed, and the pivot arm was vibrated to minimize friction due to the o-ring seals.

Flow Instrumentation

A thin plate orifice meter was used to measure the mass flow. The orifice was located in the vertical arm to eliminate any effects of a leak at the hinge point on the mass flow measurement. The meter was built using ASME standards (Ref. 1) with a diameter ratio of .50. ASME guidelines for pressure and thermocouple taps were followed. Fig. B-2 gives the details.

The mass flow meter required pressure readings before and after the orifice. A 0-1000 psig Statham pressure transducer measured the upstream pressure and a 0-500 psig Statham pressure transducer measured the downstream pressure. For very low mass flows, a ±5.0 psid Statham pressure transducer was used in conjunction with the 0-500 psig transducer for greater accuracy. A copper-constantan thermocouple was located downstream to complete the mass flow meter instrumentation.

The stilling chamber pressure was measured using a 0-500 psig Statham transducer and a copper-constantan

thermocouple measured the chamber temperature. For the thermocouples, an ice bath was used as a reference junction. A pressure gauge was also connected to provide an easy-to-see indication for adjusting the pressure during runs. The atmospheric or ambient pressure was given by a barometer located in the test room.

A Honeywell visicorder, model 1508, was used to record the six channels of data. Each channel was wired separately with the required series and shunt resistors hardwired into the visicorder. M100-350 galvonmeters were used on all channels, and the data was recorded on eight-inch, light sensitive paper.

Clustered Nozzles

The nozzles were designed in the previous study (Ref. 5) using one-dimensional nozzle theory. Each nozzle had a nozzle area ratio of 3.0 which corresponds to an exit mach number of 2.63 and an exit-to-chamber pressure ratio of .0478 (see Fig. B-3).

For ease of comparison, the total throat area was held constant for the original study (Ref. 5) where two-nozzle, four-nozzle and six-nozzle clusters were considered. For this study, four additional nozzles of the six cluster size were added to form a ten-nozzle cluster. Table II lists the fully flowing nozzle configurations tested in this study. An explanation of the numbering system is given below the table. The total throat area of the ten-nozzle cluster was 1.67 times the total throat area of the other clusters.

This allowed some nozzles to be sealed and yet maintain the standard total throat area. The ten-nozzle cluster was only tested at low pressures in the full-flowing condition due to compressed air requirements. Each nozzle was machined separately and attached to a back plate with screws. Single nozzles of each individual nozzle size and a large single nozzles of the same total throat area as the clusters were used to establish baseline data.

To determine the effects of an inoperable nozzle on the performance of a cluster, nozzle plugs were made for each individual nozzle size. The details were shown in Fig. B-3. The plug was held in place by a screw running through the throat area with an o-ring sealing the high pressure side. For each cluster configuration the location of sealed nozzles could be varied. Table III lists the cluster configurations tested. The X-prefix indicates the configuration contains at least one sealed nozzle.

Aerodynamic shrouding was studied by using clay to mold an aerodynamic shroud around the two-nozzle, four-nozzle and six-nozzle clusters. This provided a smooth transition from the back plate to the exit of the nozzles. No gap was allowed between the shroud and the nozzles for air to flow into. Fig. 4 shows the shrouds.

Table II Fully Operating Nozzle Configurations

Nozzle Name	Configurations	At(in^2)
01		.2945
02		.1472
03		.0736
04		.0491
2-2		.2944
3-4		.2944
4-6		.2945
4-10		.4908
S2-2		.2944
S3-4		.2944
S4-6		.2945

Notation:

S 4 - 6

- 6: number of nozzles in configuration
- 4: single nozzle size
- S = shroud

Table III Nozzle Configuration
with Non-Operating Nozzles

Nozzle Name	Configuration	At (in^2)
X2-2		.1472
X3-4		.0736
XX3-4-2		.1472
XX3-4-2		.1472
X4-10-1		.2945
X4-10-2		.2945
XX4-10-1		.0982
XX4-10-2		.0982
XX4-10-3		.0982
XX4-10-4		.0982

○ - operating nozzle

● - non-operating nozzle

Notation:

XX4-10-3

- 3 — number of configuration in particular series
- 10 — number of nozzles in configuration
- 4 — single nozzle size
- XX — X or XX implies configuration has inoperable nozzle

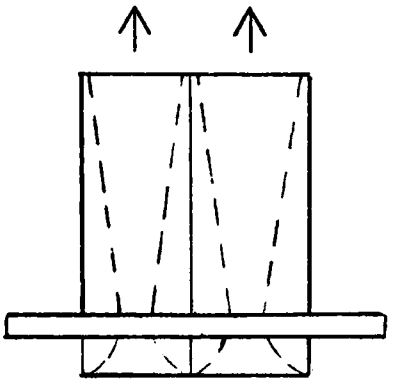

Nozzle 2-2

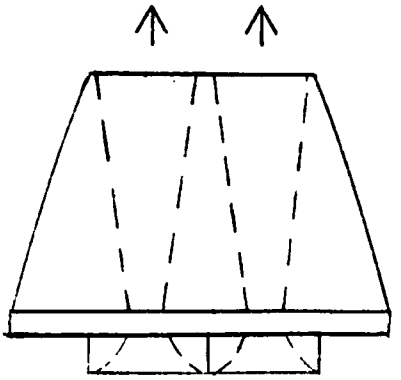

Nozzle S2-2

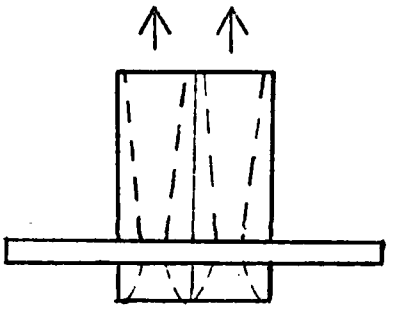

Nozzle 3-4

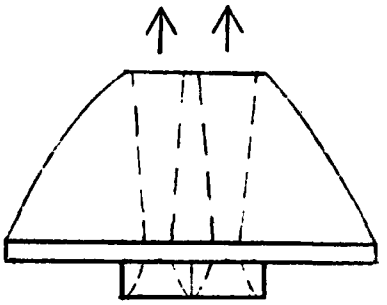

Nozzle S3-4

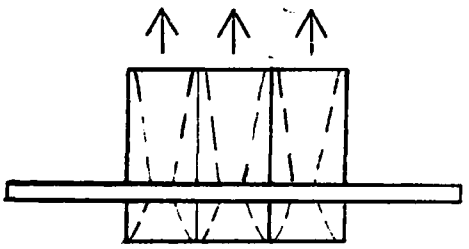

Nozzle 4-6

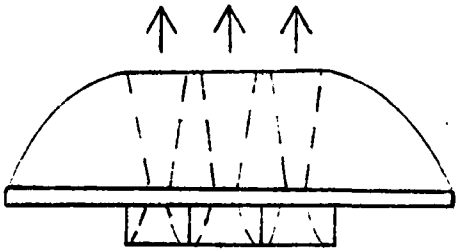

Nozzle S4-6

Figure 4. Aerodynamic Shrouds on Clusters

III Experimental Procedure

The experimental procedure consisted of calibrating the instrumentation and running the tests. Calibration was performed approximately every two weeks.

Calibration

All the psig pressure transducers were calibrated using an Ashcroft dead weight tester. The calibration was done in 50 psi increments from zero to 450 psig. The 450 psig limit was required for the upstream flowmeter transducer. The psid transducer was calibrated using a specially built pressurization system, which is shown in Fig. B-4. The system allowed a 0 - 15 psi pressure differential across the transducer while maintaining a line pressure of 350 psig. This permitted simulating the actual test conditions at the highest pressure used in the investigation.

The copper-constantan thermocouples were calibrated using 32F as one reference point and the temperature of boiling water as the other. A slope of millivolts versus chart deflection was determined from the calibration. The millivolts were converted to degrees by using a thermocouple conversion table.

The thrust measuring system was calibrated using calibrated weights. The cantilever aluminum force beam was removed from the thrust stand and clamped in a horizontal position with the thrust bolt point upwards. The weights were hung directly on the bolt by the use of a specially

built weight holder. This eliminated friction as a factor. A slight hystersis effect was noticed when a data point was approached from the high side as opposed to being approached from the low side. The thrust measurement system was calibrated at several different excitation voltages, in order to obtain the greatest accuracy as possible for the particular nozzle configuration being tested. The output was linear with excitation voltage. The excitation voltages used were 3.0, 5.0 and 8.0 volts, and the output slopes were 21.33, 12.80 and 8.0 lb_f/in respectively.

Test Procedure

For each configuration to be tested, the correct transducer set-up had to be selected. For most cases, this was the 0-1000 psig and 0-500 psig transducer set-up for the pressure differential measurement at the mass flowmeter. Only the two small single nozzles required the psid transducer instead of the 0-1000 psig transducer. The correct strain gauge excitation voltage was selected depending on the configuration and testing pressure. Testing was done in a series of five runs. Data was taken at tank pressures of 150, 200, 250, 300 and 350 psig. This pressure range caused the nozzles to be operated at both overexpanded and underexpanded conditions. At least two series of runs were accomplished for each configuration. Each pressure data point was approached from below to avoid the hystersis effect in thrust measurement. At the start of each test day, the pressure transducers were exercised by quickly

running up the pressure and then venting it several times. This made the transducers' response more repeatable.

After the six data channels were recorded by the visicorder, the five runs would be reduced together. The data was reduced as quickly as possible to reduce the effect of paper aging on the deflection readings. The actual deflections were converted to physical data (psig, F, lb_f) by the use of calibration slopes. A programmable calculater reduced the data into mass flows and thrust coefficients.

IV Results and Discussions

Twenty-one different nozzle configurations were tested. For each nozzle configuration the thrust coefficient was plotted against the pressure ratio as an indication of the performance. Appendix A contains a separate plot for each configuration along with the curve based on theory. Appendix A also includes some additional comparisons of different nozzle configurations. A computer generated second-order curve fit was used to draw the measured thrust coefficient data curve. The theoretical curve is based on equation (3). Table IV lists the measured thrust coefficient for all the configurations at the optimum expansion ratio and compares them to theory.

Single Nozzles

The single nozzles are compared to each other in Fig. A-1 and individually to theory in Fig. A-10 through Fig. A-13. The single nozzles performed within 2% of the theoretical values through the pressure ratio range tested. Viscous effects would be the greatest at nozzle 04 due to it being the smallest, but as Fig. A-13 shows, the actual performance matches up very well with the predicted theoretical performance. Therefore, viscous effects can be assumed to be negligible. Except for one point for nozzle 03, all the data points are within a 2% spread. This indicated a very high degree of repeatibility (98%). Along with the good agreement with theory,

the repeatability of the data provides a good basis for confidence in the data.

Full Flow Nozzle Clusters

Fig. 5 compares the three fully operating clusters with the large single nozzle, nozzle 01. Nozzle 2-2 shows a 2% increase in the performance at the lowest pressure ratio but drew nearer to the single nozzle as the pressure ratio increased. Throughout the pressure ratio range tested, there was no noticeable difference between nozzle 3-4 and nozzle 01. A comparison of nozzle 4-6 and nozzle 01 shows a single nozzle outperformed the cluster by up to 2% at the higher pressure ratios. Nozzle 4-10 could only be tested up to a pressure ratio of fifteen and was not included in the comparison. Overall, the clusters did not perform consistantly better or worse than the single nozzle and the differences were within the error margin of approximately two percent. Fig. 6 contains Schlieren photographs of nozzle 3-4 operating with two nozzles sealed for a clearer picture. In both the overexpanded and underexpanded cases, the two flows do not interact with each other. Each individual flow stream appears to be acting as a single nozzle. This would agree with the Goethert study (Ref. 3) which said a nozzle-exit-to-ambient pressure ratio of ten or more is required for the interaction of two flow streams, which is necessary for an effect on performance. The highest run pressure, 350 psig, only provided a nozzle-exit-to-ambient

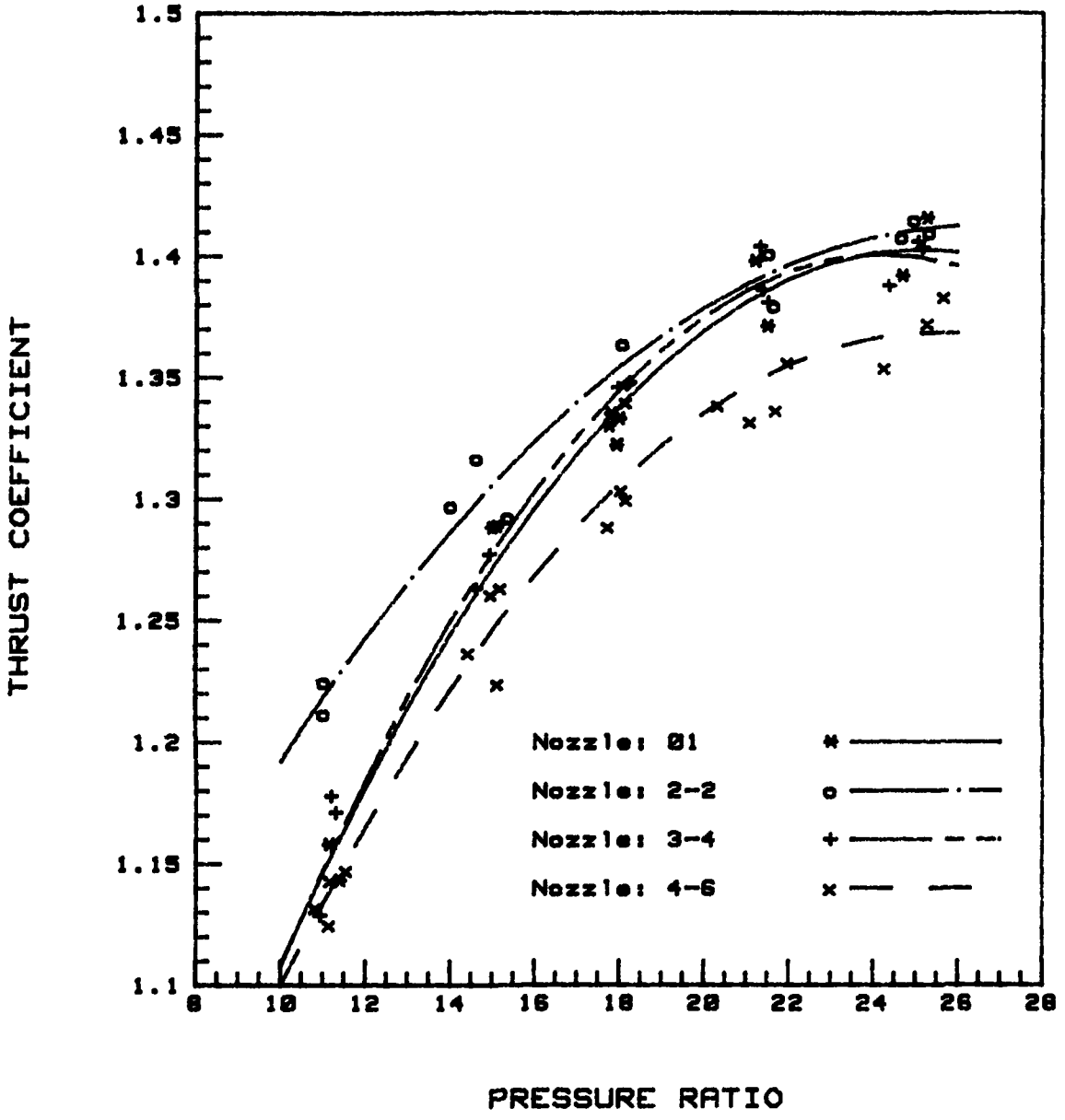

FIG 5. Performance Comparsion of
Cluster Nozzles and Nozzle 01.

a) Overexpanded Flow
(PR=11)

b) Underexpanded Flow
(PR=25)

Figure 6. Schlieren Photographs of Nozzle XX3-4-2

pressure ratio of 1.20 due to the high ambient pressure at sea level.

Comparing a cluster to the single nozzle of the same individual nozzle size (i.e. nozzle 3-4 vs. nozzle 03) yields basically the same result the comparison with nozzle 01 did. The comparisons are shown in Fig. A-1 through Fig. A-3. The only major difference was the large amount nozzle 04 outperformed nozzle 4-6 in the underexpanded region. The reason for the seven percent difference is unclear, but the difference was repeatable.

Cluster Configuration with Non-Operating Nozzles

Comparisons of a cluster configuration with only a single nozzle flowing (nozzles X2-2 and X3-4) to a single nozzle of the same total flowing throat area (nozzles 02 and 03) are given in Fig. A-5 and Fig. A-6. They show the cluster configuration and the single nozzle perform equally well at the lower pressure ratios (greatly overexpanded), but the cluster falls behind as the pressure is increased. This causes the thrust coefficient curves for the clusters to be flatter.

Nozzles XX3-4-1 and XX3-4-2 were tested to see the effect of location of inoperable nozzles on a cluster. Nozzle XX3-4-1 had sealed diagonal nozzles, while nozzle XX3-4-2 had adjacent sealed nozzles. As Fig. A-7 shows, there was very little difference in the performance of the two configurations except for a slight difference in slopes in the overexpanded regime. If there is no interaction taking place, the two configurations should be equal in performance.

Nozzles X4-10-1 and X4-10-2 had the same total throat area as nozzle 4-6. Nozzle X4-10-1 had all six flowing nozzles together to maximize any potential clustering effects, while nozzle X4-10-2 separates the open nozzles from each other by placing the sealed nozzles in between the open nozzles and thereby minimizing the clustering effect. Comparing the two nozzles in Fig. 7 indicates no appreciable difference in performance between the two configurations. This verified the results that clustering doesn't have any effect at the pressure ratios tested at ambient pressure.

The ten nozzle clusters with only two flowing nozzles (nozzles XX4-10-1, XX4-10-2, XX4-10-3 and XX4-10-4) showed a significant increase in performance over theory. The four nozzle clusters are compared to theory in Fig. 8. The difference in performance increases with pressure and reaches its maximum in the underexpanded region. At a pressure ratio of 24, the clusters outperform theory from 3.6% (XX4-10-1) up to 5.4% (XX4-10-3). The error margin cannot account for such a great increase in performance, and the increase is consistant with all four clusters. Fig. 9 shows Schlieren photographs of this basic configuration (actually XX4-10-3), and, as before, there is no interaction of individual jets. There is a must greater amount of base plate area right at the nozzle exit plane with this configuration. The physical phenomenon responsible for the increase is not known at the present time.

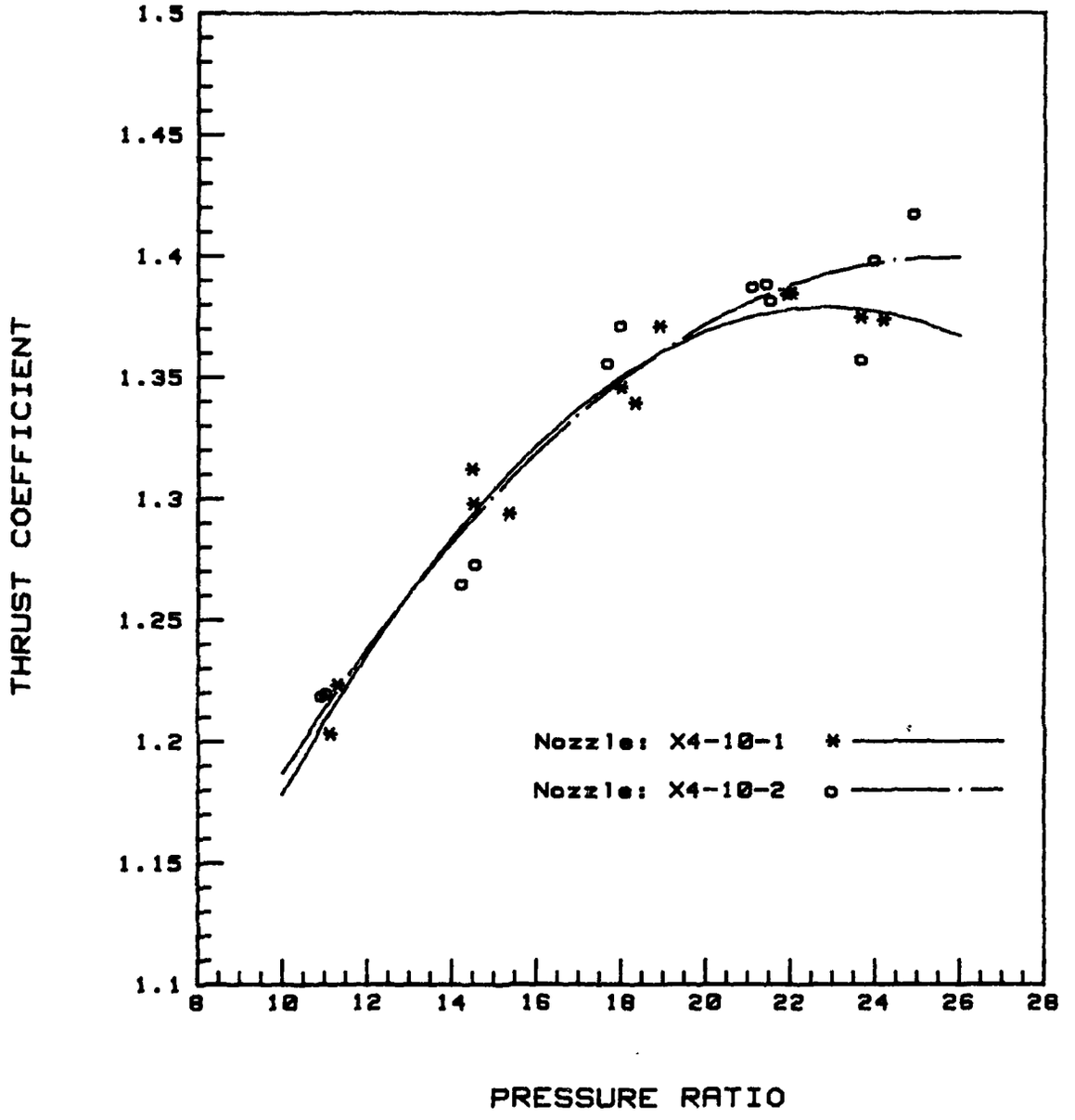

FIG 7. Performance Comparsion of
Nozzle X4-10-1 and Nozzle X4-10-2.

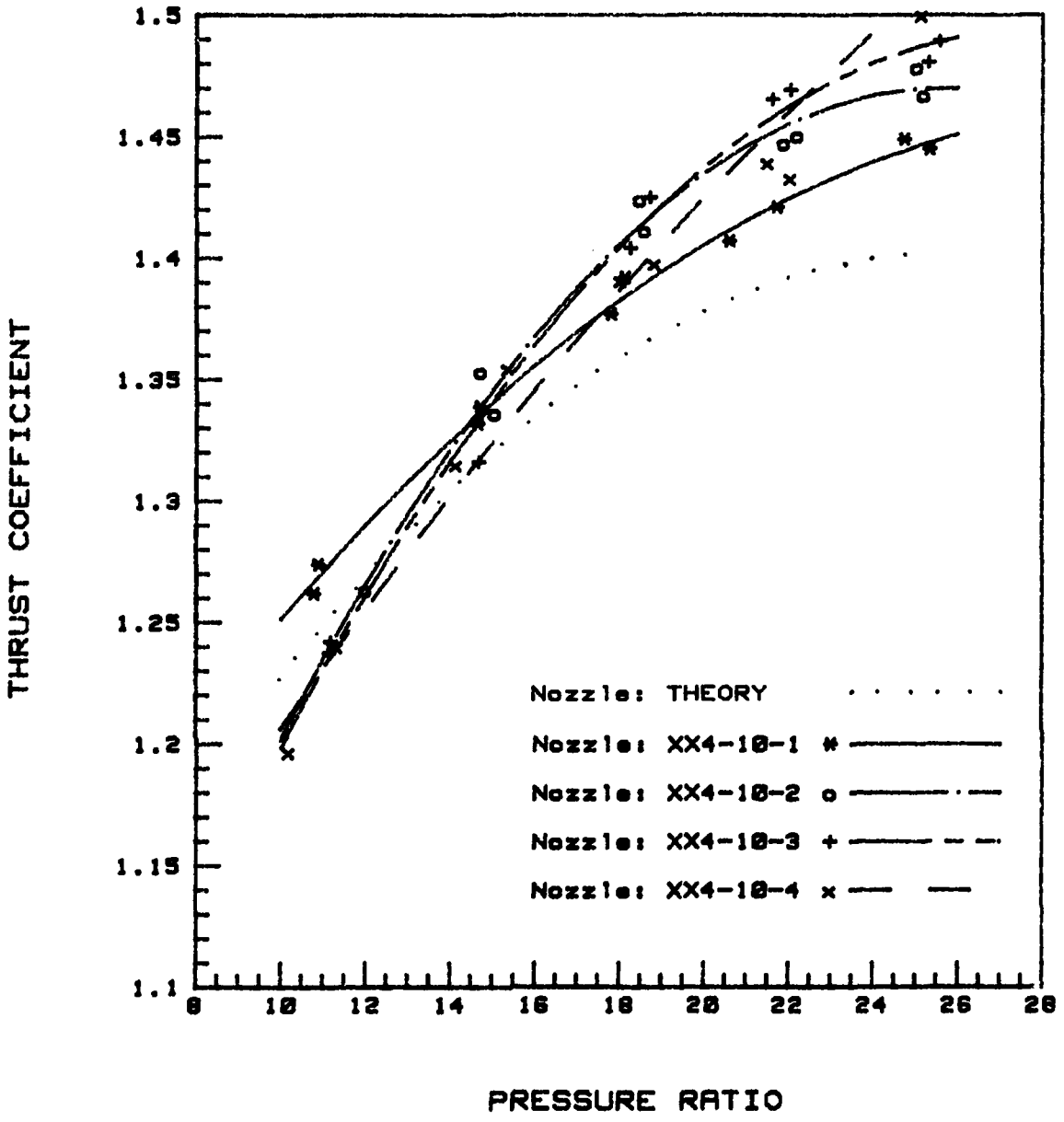

FIG 8. Performance Comparsion of Nozzles XX4-10-1, XX4-10-2, XX4-10-3 and XX4-10-4.

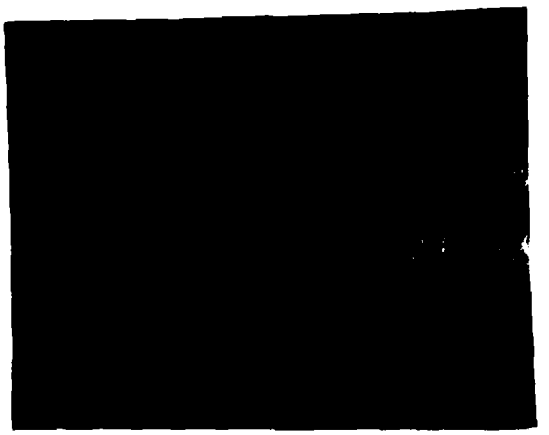

a) Overexpanded Flow
(PR=11)

b) Underexpanded Flow
(PR=25)

Figure 9. Schlieren Photographs of
Nozzle XX4-10-3

Shrouded Cluster Configurations

The placing of an aerodynamic shroud on the cluster configurations seem to slightly decrease their performance. Fig. 10 shows the performance decrease by comparing nozzle S3-4 and nozzle 3-4. Fig. A-8 and Fig. A-9 compares the other two shrouded nozzles to their unshrouded counterparts. The decrease in performance only ranges from 1.0% (nozzle S4-6) to 3.6% (nozzles S3-4), but the fact that all three cases show a decline in performance is significant.

A possible explanation is that the aerodynamic shrouding decreases the effect of the nozzle base plate area on the performance by allowing a smoother transition to the base plate. This would modify the flow at base plate and could lead to a thrust decrease.

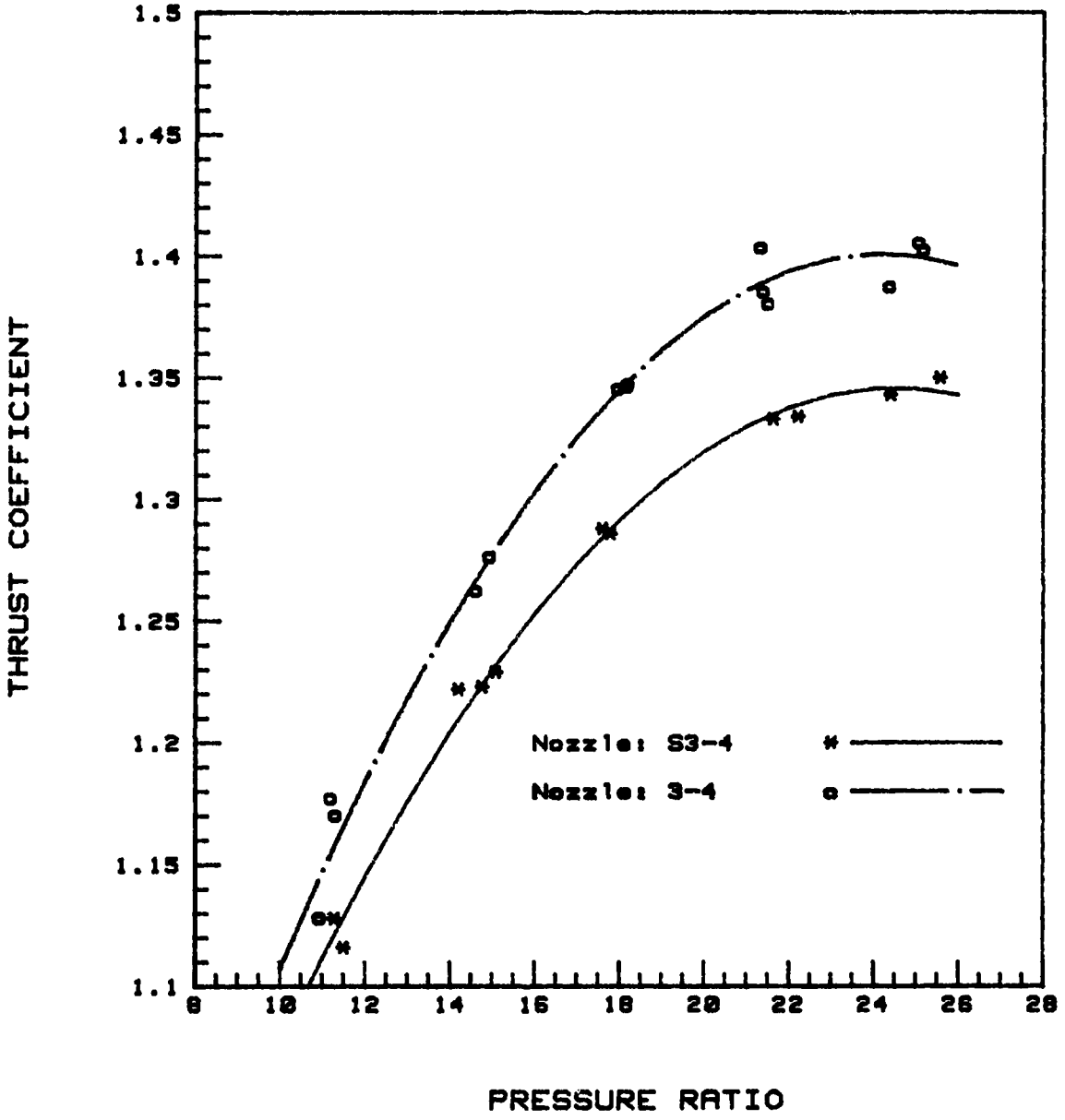

FIG 10. Performance Comparsion of Nozzle S3-4 and Nozzle 3-4.

V Conclusions

Nozzle clusters containing up to ten nozzles were cold flow tested and compared with a single nozzle of the same total throat area. Then individual nozzles in clusters were sealed, and the partially operating nozzle clusters tested. Finally, the effect of aerodynamic shrouding on nozzle clusters was experimentally studied. Results of these tests conducted at ambient conditions lead to the following conclusions:

1. At ambient conditions, the clustering of nozzles does not effect the performance of the individual nozzles to any significant degree at the pressure ratios tested. The nozzle-exit-to-ambient pressure ratio is not large enough for any interaction between individual jets.

2. An inoperable nozzle in a cluster does not effect the performance of the remaining flowing nozzles in a cluster except when the base plate area has been significantly increased. It also follows that the location or pattern of sealed or operable nozzles has no effect on the flowing nozzles performance due to lack of interaction.

3. The placing of an aerodynamic shroud (with no open space between the nozzle and shroud) results in a slight decrease in performance as it does decrease any potential effect of the base plate on the flow.

VI Recommendations

Nozzle clusters were tested at sea level conditions and at moderate pressures (150-350 psig) for this study. The effects of inoperable nozzles and aerodynamic shrouded nozzles were also investigated. The above testing and examination of the results of the testing gives rise to the following recommendations for further work in the study of cluster nozzles.

1. The above testing should be done at simulated high altitude (above 60,000 feet). At high altitude, the exhaust will be greatly underexpanded and will cause the jets from different nozzles to interact. To accomplish this at sea level, a tank pressure of over 2500 psi would be required. If simulated high altitude cannot be done, no further testing is warranted. The following recommendations are based on being able to test at simulated high altitude.

2. Various patterns of nozzles should be tested. Potential patterns include circular, oval and circular with a center nozzles.

3. Shrouding with spacing between the shroud and the nozzle should be tested to see the effect of the shroud on the entrapment of air caused by the interaction of exhaust jets at high altitudes.

4. Testing of shrouding that would allow the thrust of individual nozzles or the entire cluster to be vectored would be of great interest. This would require a thrust

stand capable of measuring loads in more than one direction.

5. For any particular application, the exact configuration should be tested as the performance of a cluster is heavily configuration geometry dependent.

Bibliography

1. Bean, Howard S. Fluid Meters: Their Theory and Application, Part II. New York: The American Society of Mechanical Engineers, 1971.

2. Etemad, G. A., Parker, G. H., and Sheeran, M. C. "Flow Characteristics, Convective and Radiative Heating in the Base Area of the Polaris Missle." Proceedings of the Simulated Altitude Testing of Rockets and Missles Components Symposium. 3-5-1--3-5-39. Arnold AFS, Tennessee: ARO, Inc., and Space Technology Laboratories, Inc., March 1960. (A.D. 316-061)

3. Goethert, Bernard H. Studies of the Flow Characteristics and Performance of Multi-Nozzle Rocket Exhausts. AEDC-TR-59-16. Arnold AFS, Tennessee: ARO, Inc., October 1959. (A.D. 313-155)

4. Harper, D. J. "The Thrust Augmentation of Rocket Motor at High Altitudes", Journal of the Royal Aeronautical Society 68. 799-807, (December 1964).

5. Hibson, D. H. "Performance Characteristics of Clustered Nozzles." M.S. Thesis, Wright-Patterson A.F.B., Ohio: Air Force Institute of Technology, December 1981.

6. Keenan, J. H. and Kaye, J. Gas Tables. New York: John Wiley and Sons, Inc. 1948.

7. Rudov, Yu M. "Analysis of Gas Flow in Multi-Nozzle Jets", Soviet Aeronautics 16 (1). 39-43. (January 1973)

8. Sutton, G. P. and Ross, D. M. Rocket Propulsion Elements. New York: John Wiley and Sons, Inc. 1976.

9. Weiss, R. R. "Non-Conventioning Configured Nozzles, for Advanced Military Spacecraft Capability." Background material to initiate study. AFRPL/LKCC, Edwards A.F.B., California, December 1980.

Appendix A

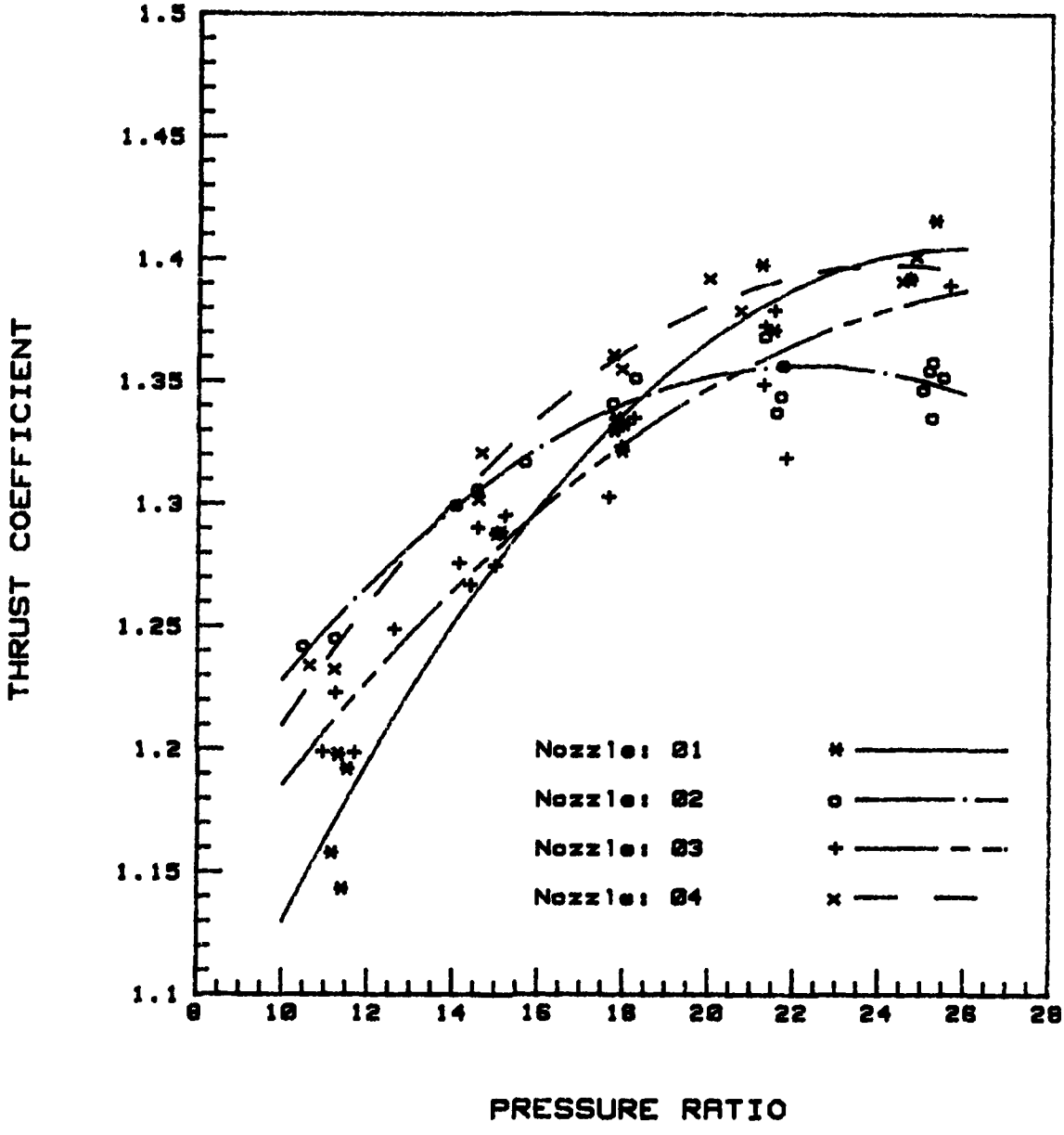

FIG A-1. Performance Comparsion of Single Nozzles.

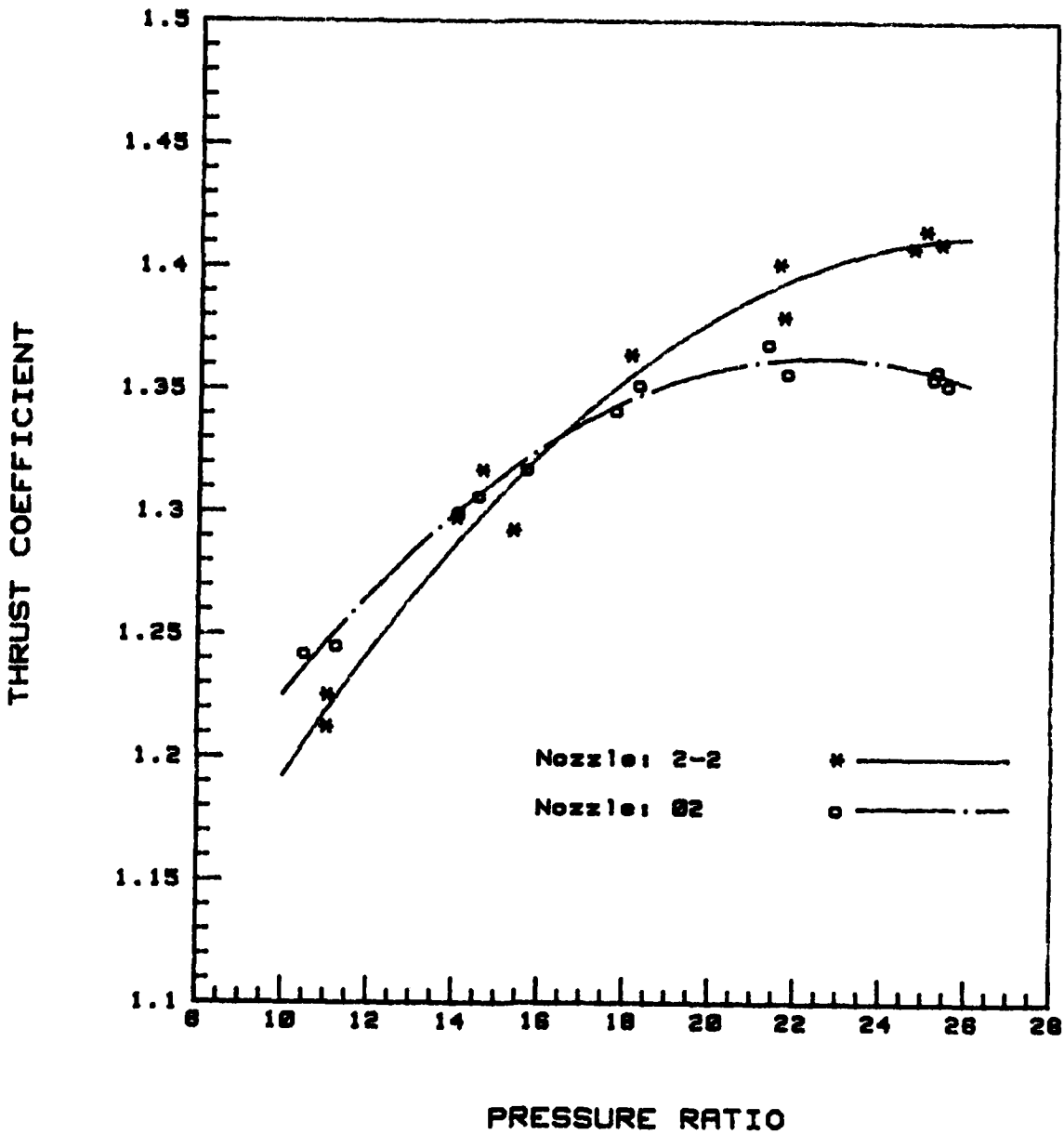

FIG A-2. Performance Comparsion of Nozzle 2-2 and Nozzle 02.

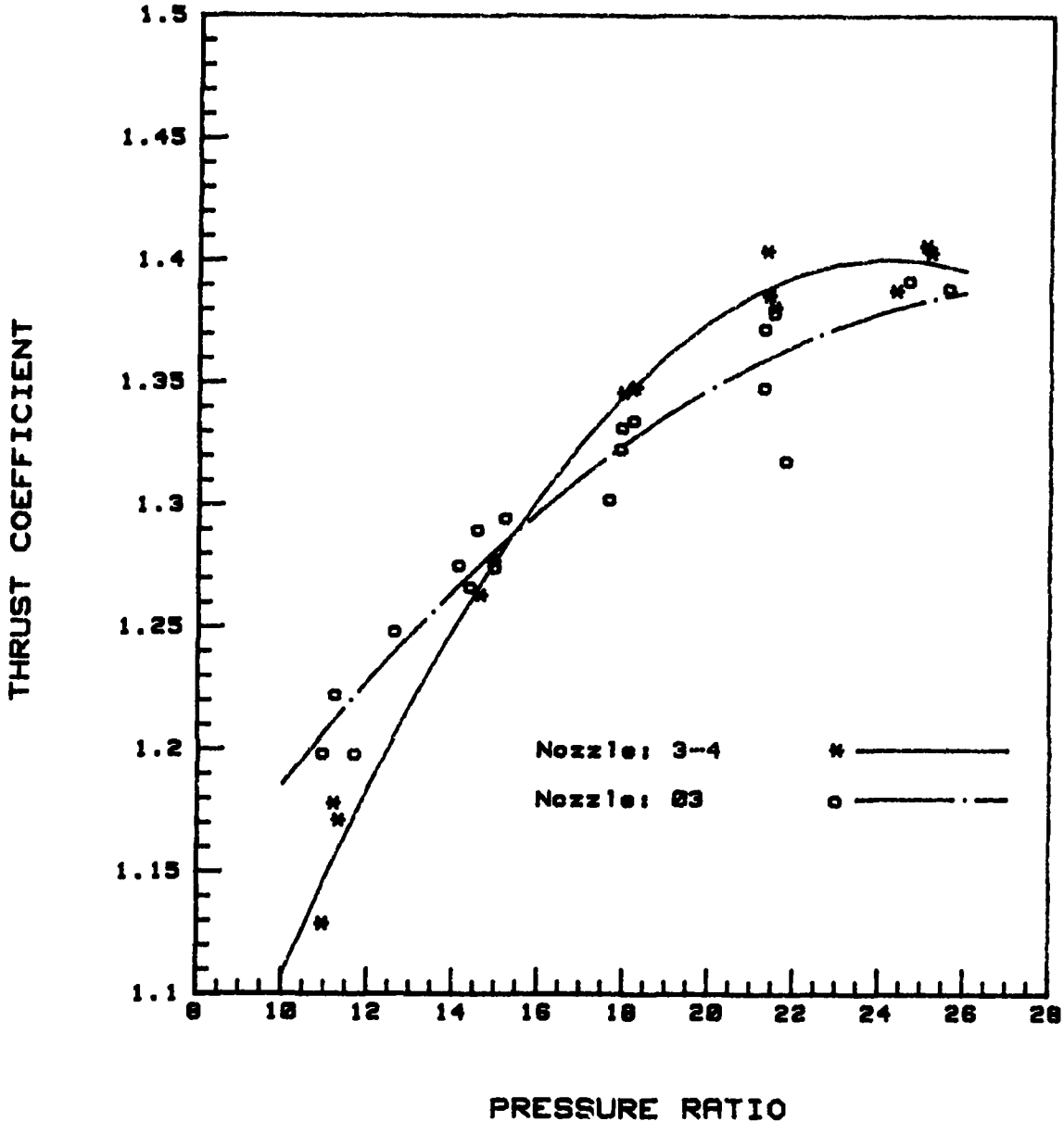

FIG A-3. Performance Comparsion of Nozzle 3-4 and Nozzle 03.

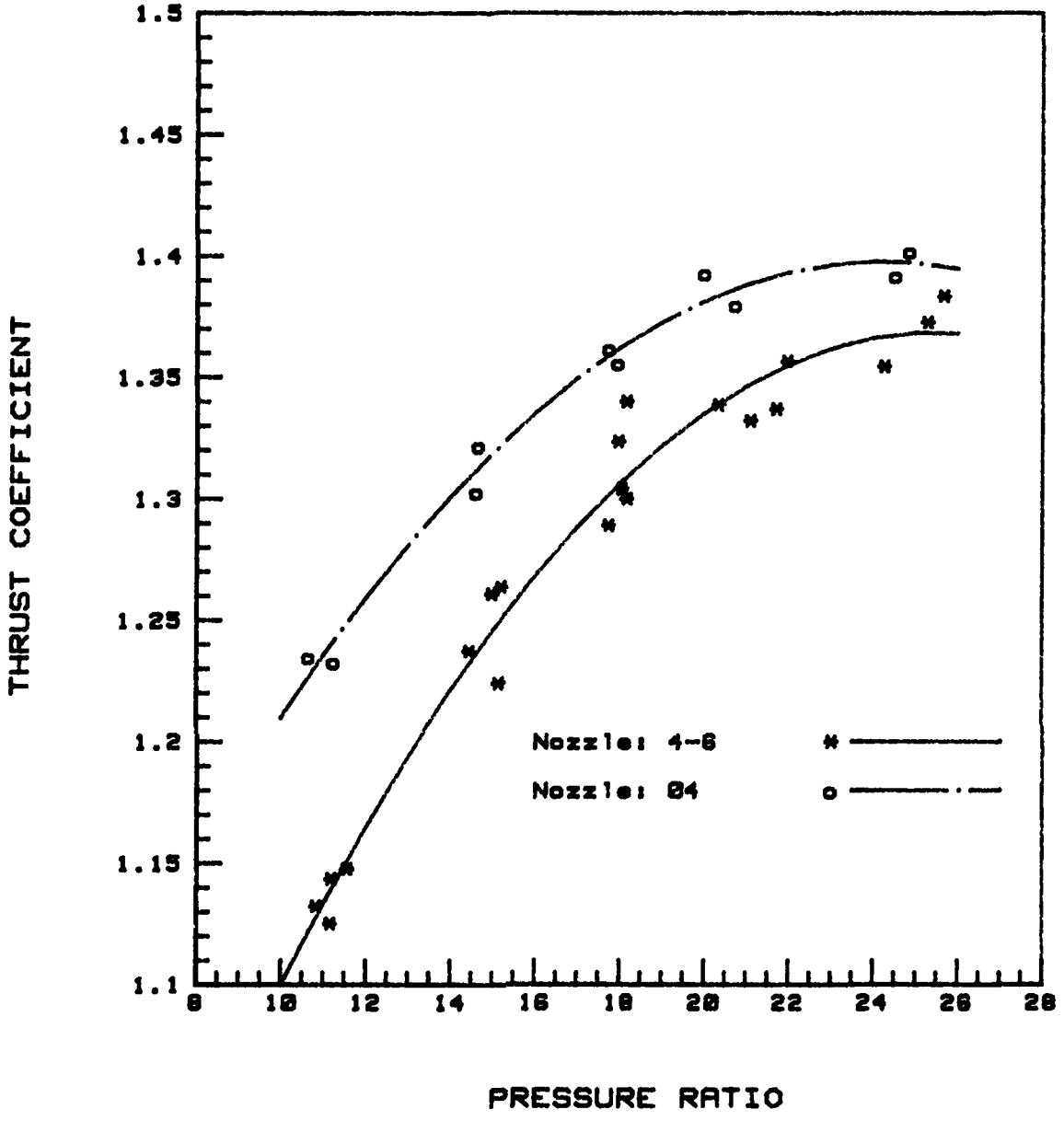

FIG A-4. Performance Comparsion of Nozzle 4-6 and Nozzle 04.

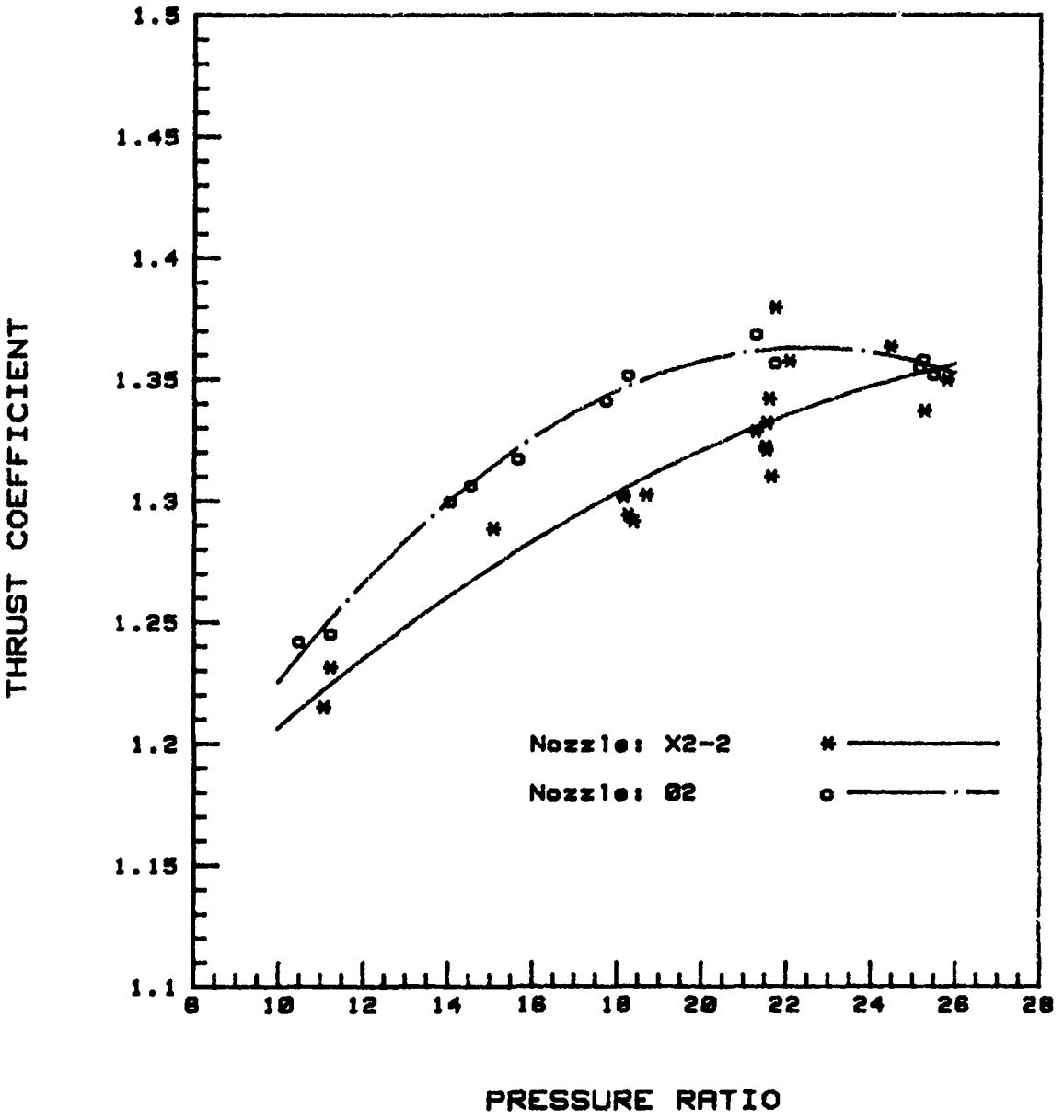

FIG A-5. Performance Comparison of Nozzle X2-2 and Nozzle 02.

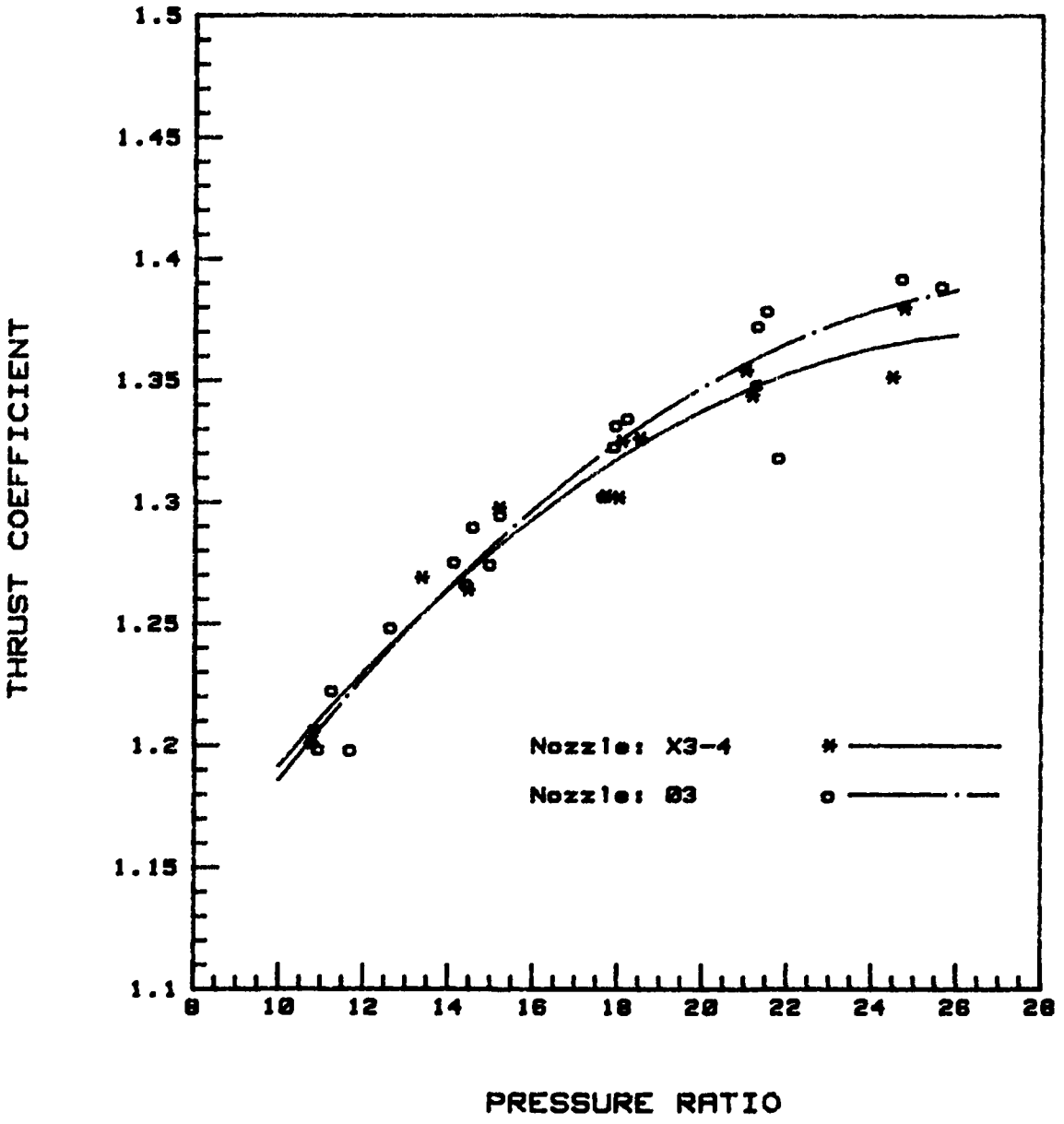

FIG A-6. Performance Comparsion of
Nozzle X3-4 and Nozzle 03.

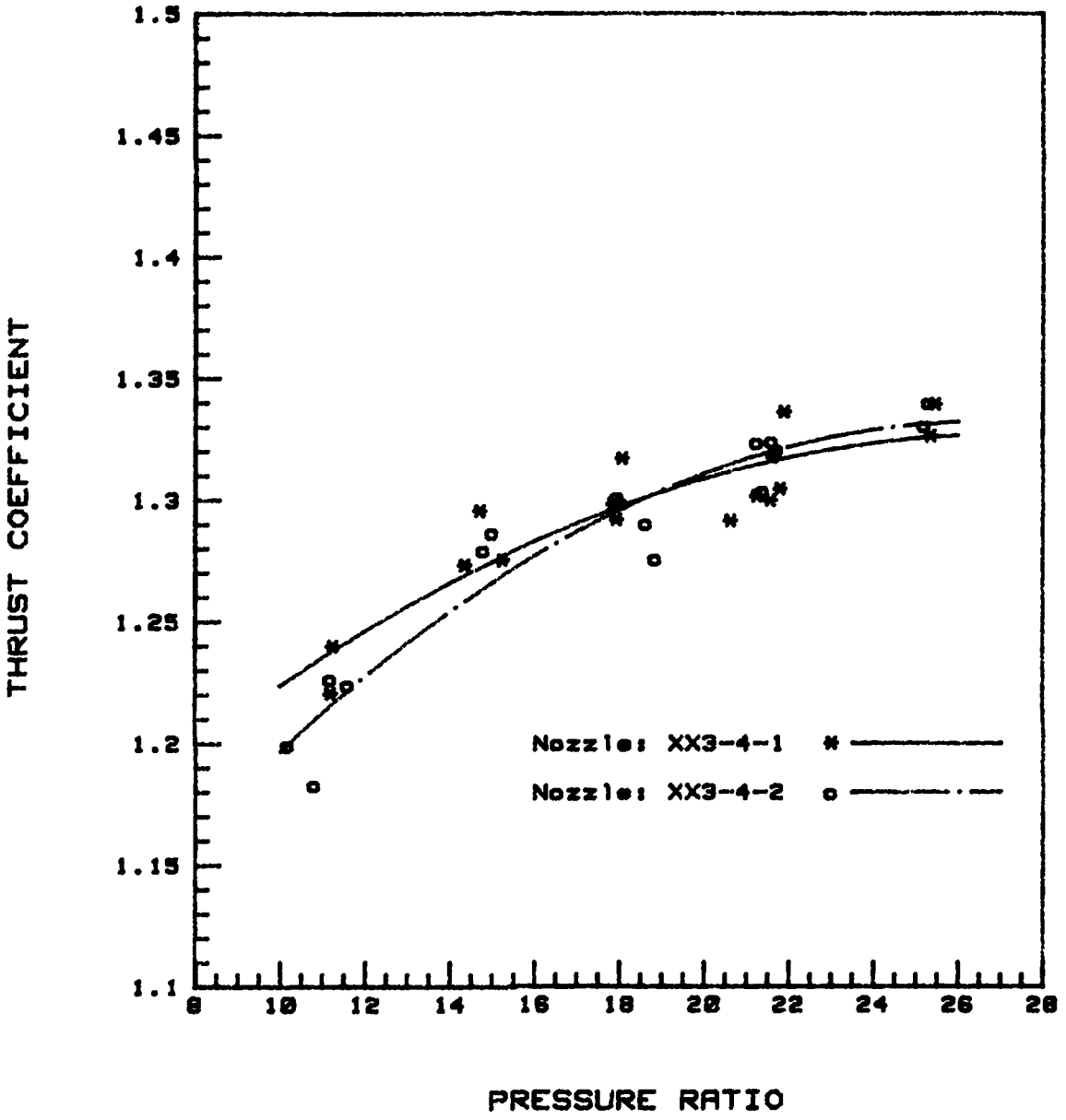

FIG A-7. Performance Comparsion of Nozzle XX3-4-1 and Nozzle XX3-4-2.

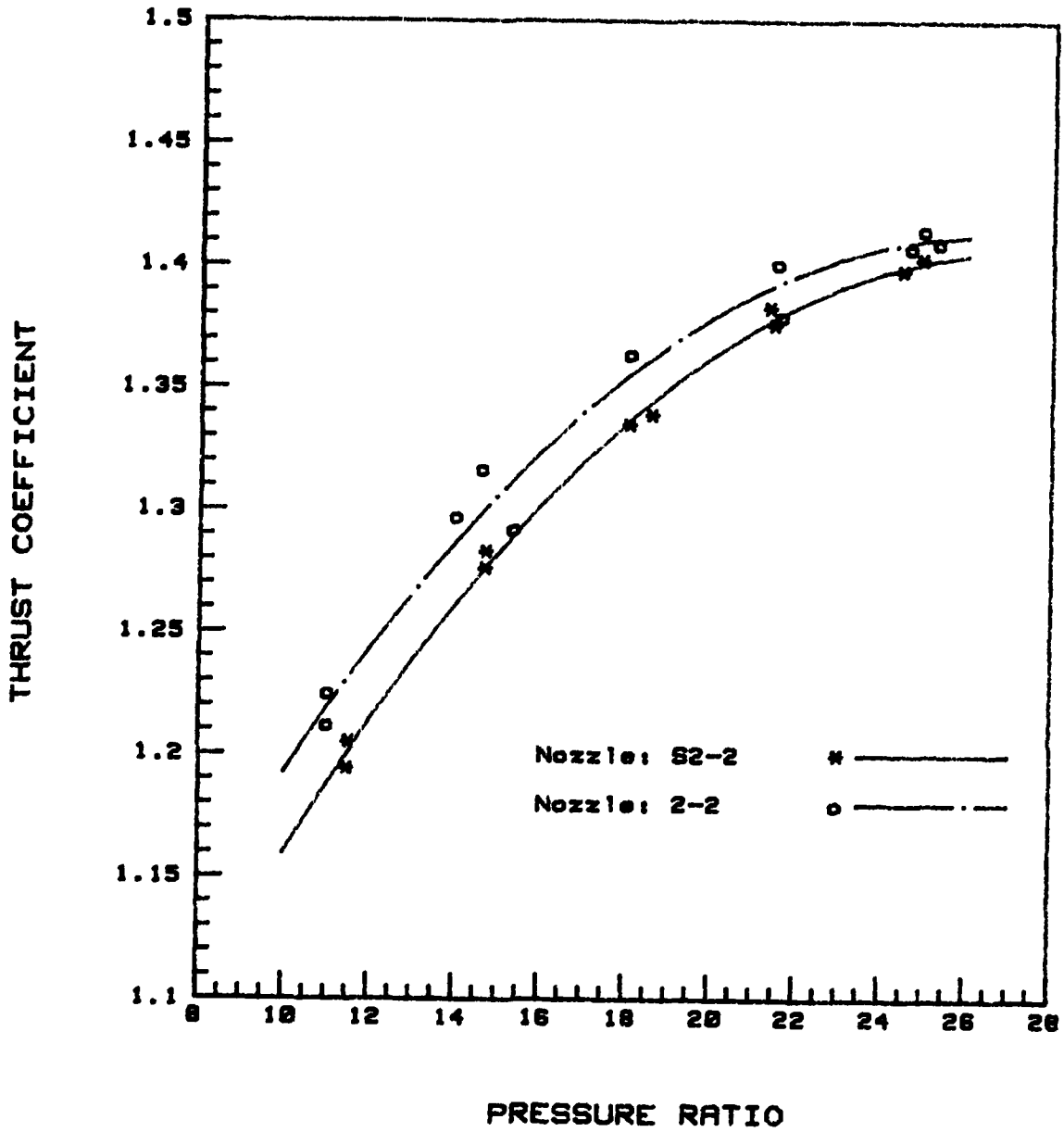

FIG A-8. Performance Comparsion of Nozzle S2-2 and Nozzle 2-2.

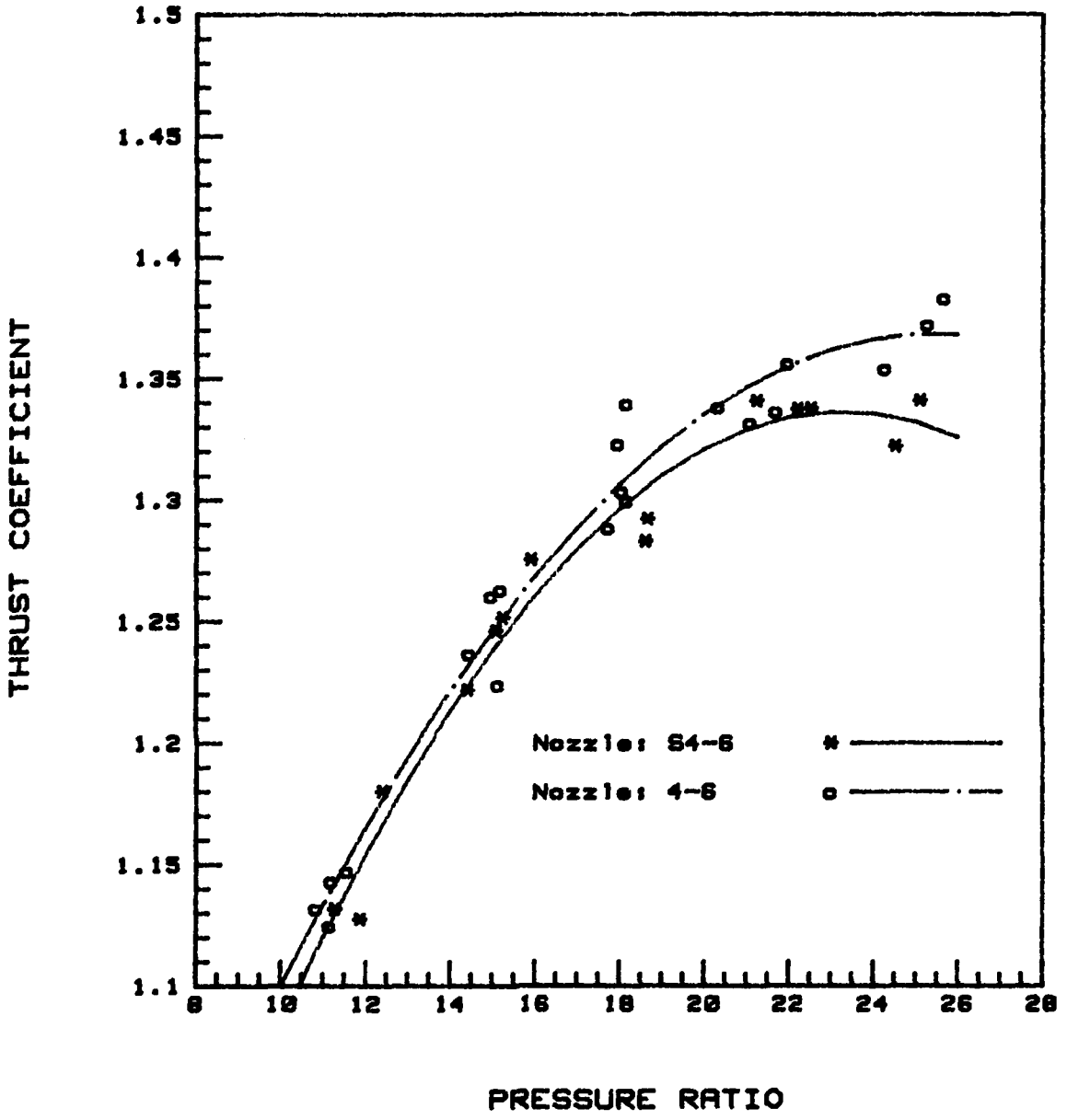

FIG A-9. Performance Comparsion of Nozzle S4-6 and Nozzle 4-6.

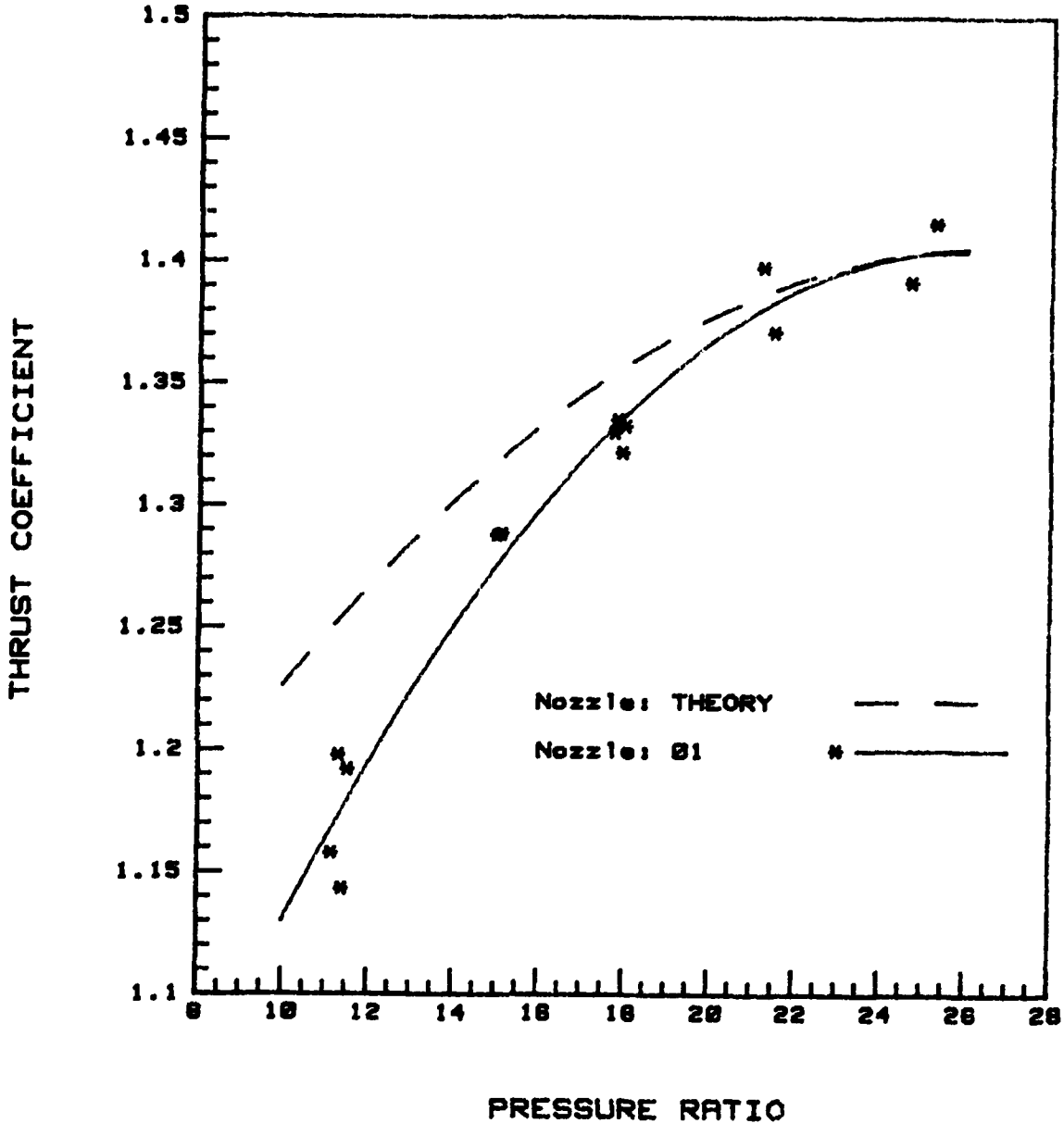

FIG A-10. Performance Comparsion of Nozzle 01 with Theory.

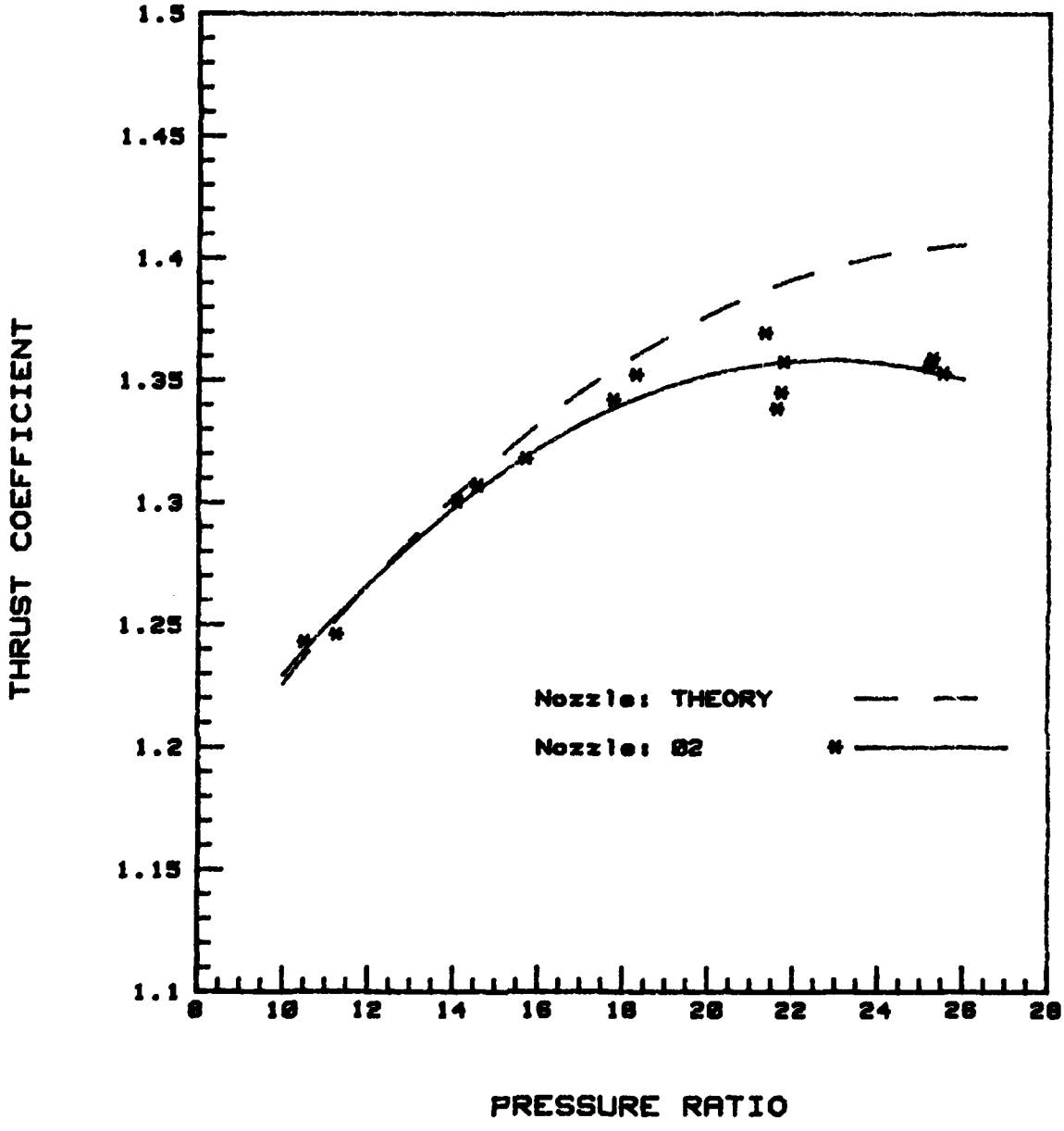

FIG A-11. Performance Comparsion of Nozzle 02 with Theory.

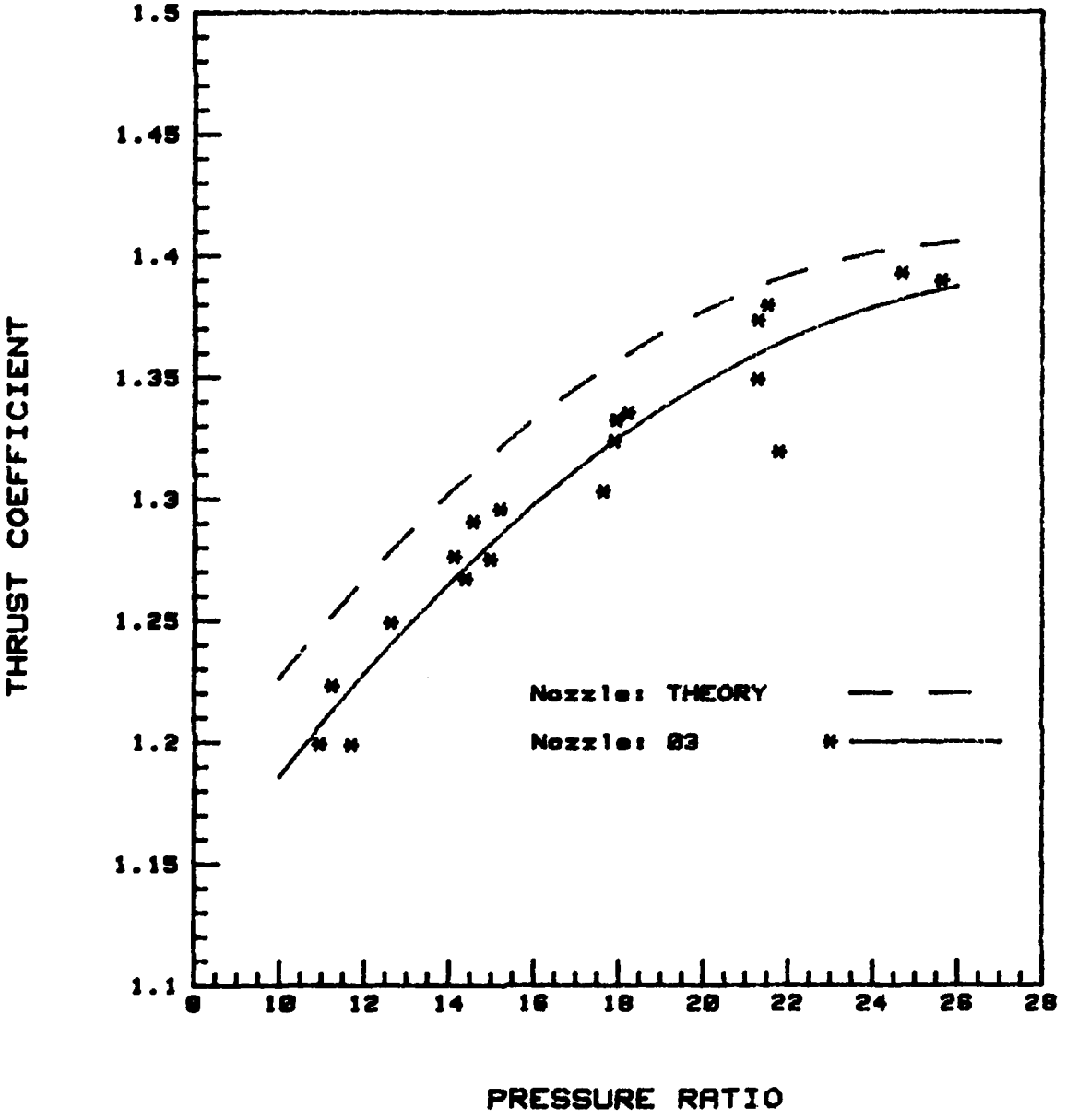

FIG A-12. Performance Comparsion of Nozzle 03 with Theory.

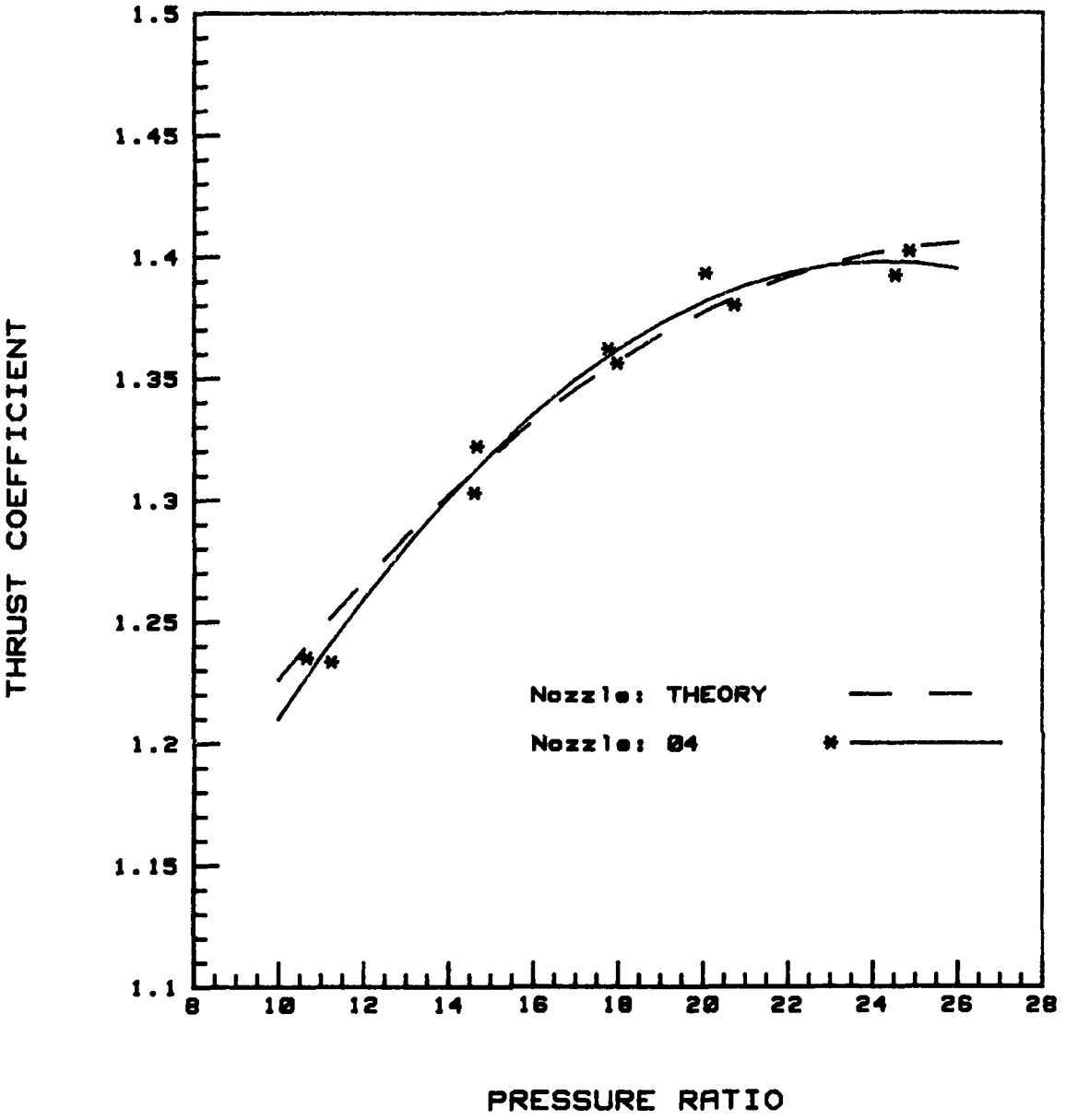

FIG A-13. Performance Comparsion of Nozzle 04 with Theory.

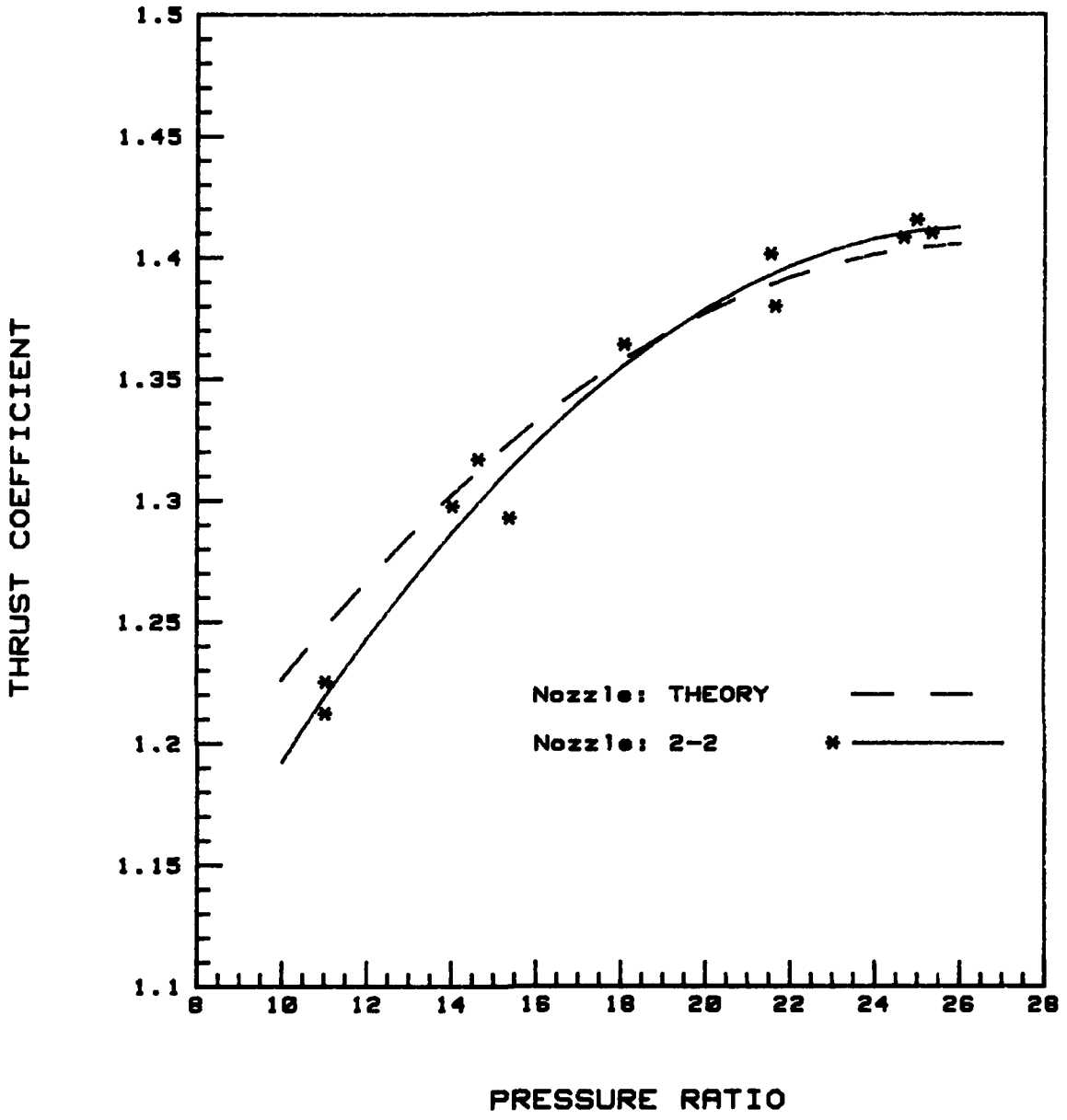

FIG A-14. Performance Comparsion of Nozzle 2-2 with Theory.

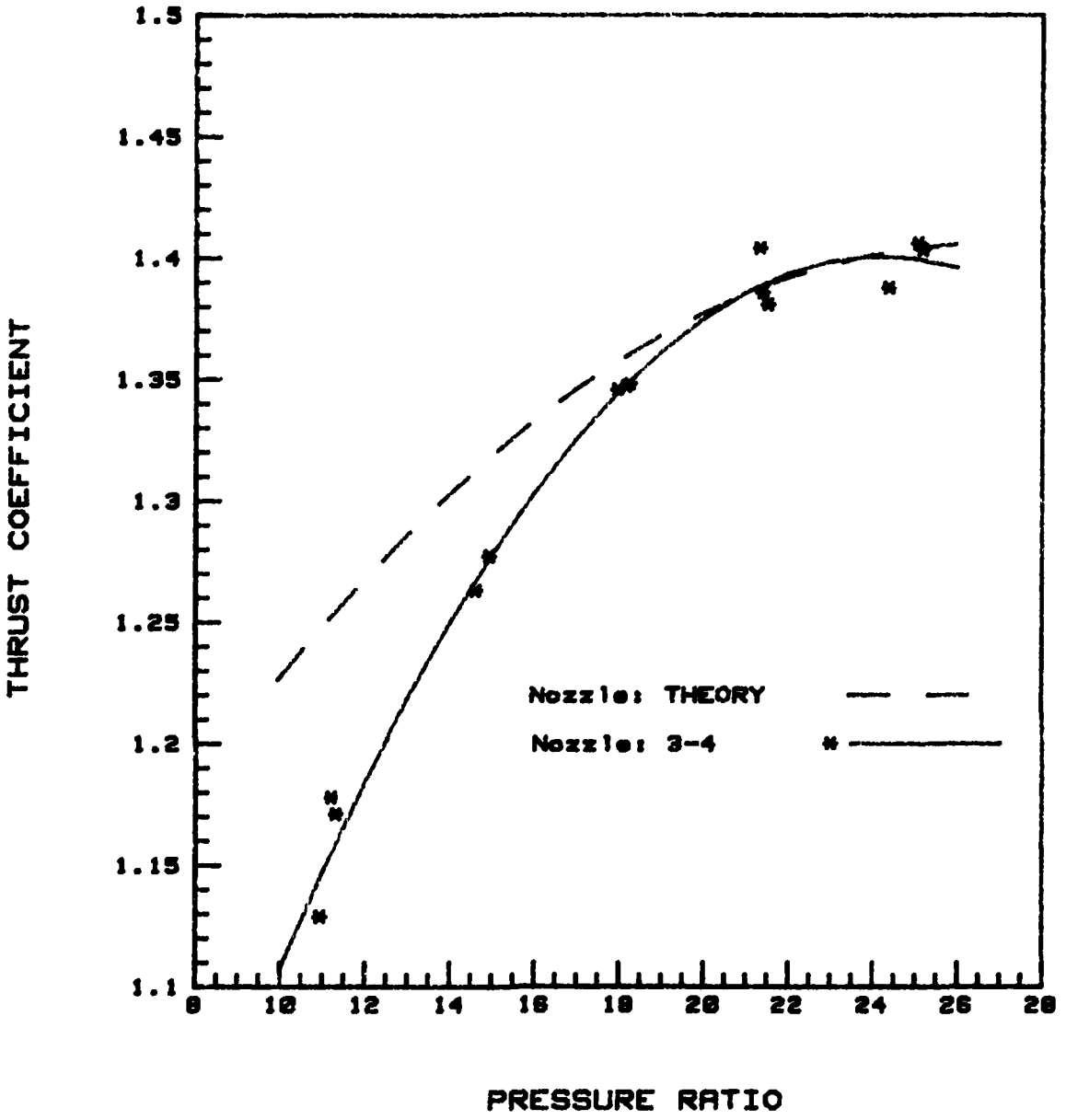

FIG A-15. Performance Comparsion of Nozzle 3-4 with Theory.

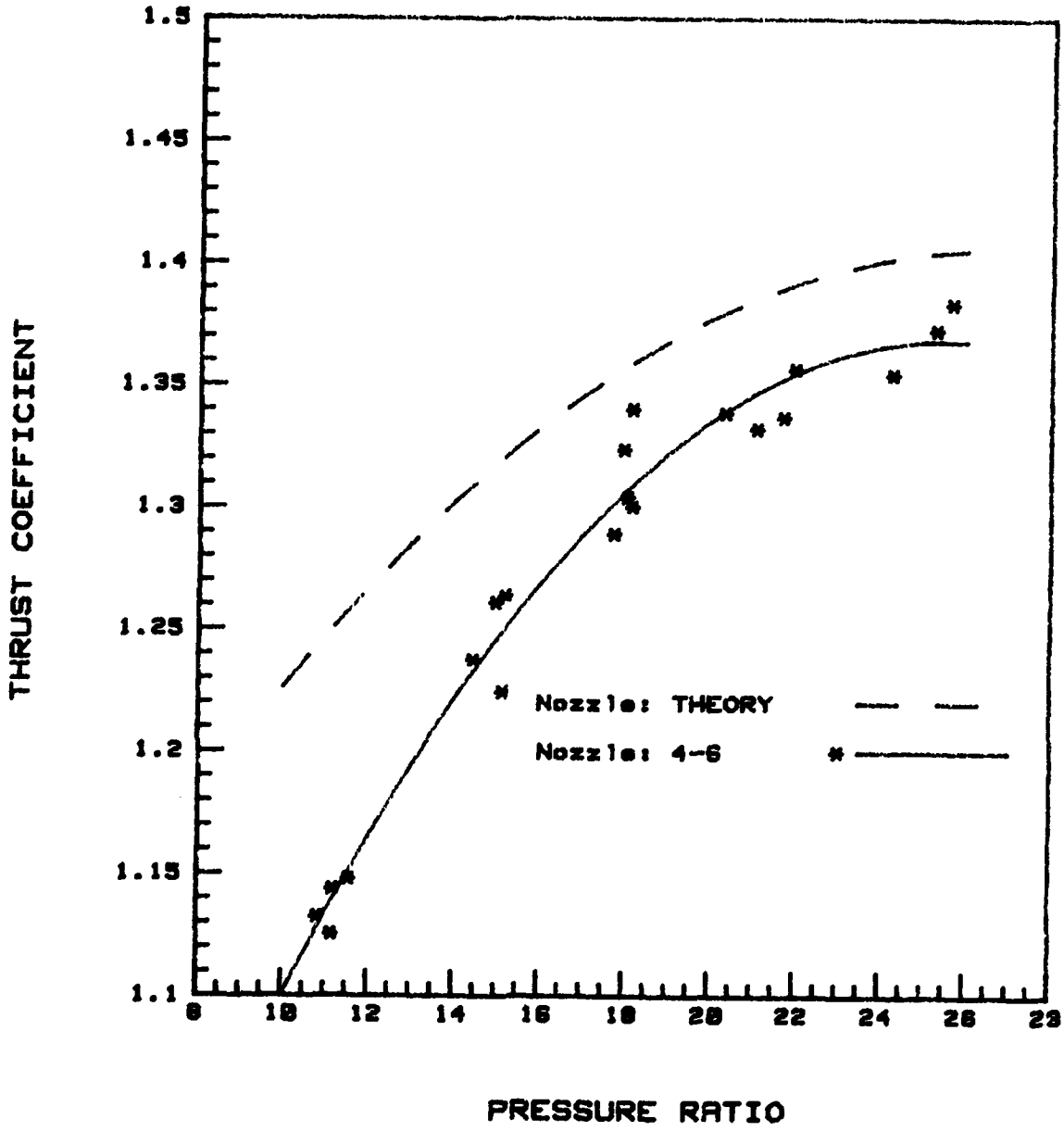

FIG A-16. Performance Comparsion of Nozzle 4-6 with Theory.

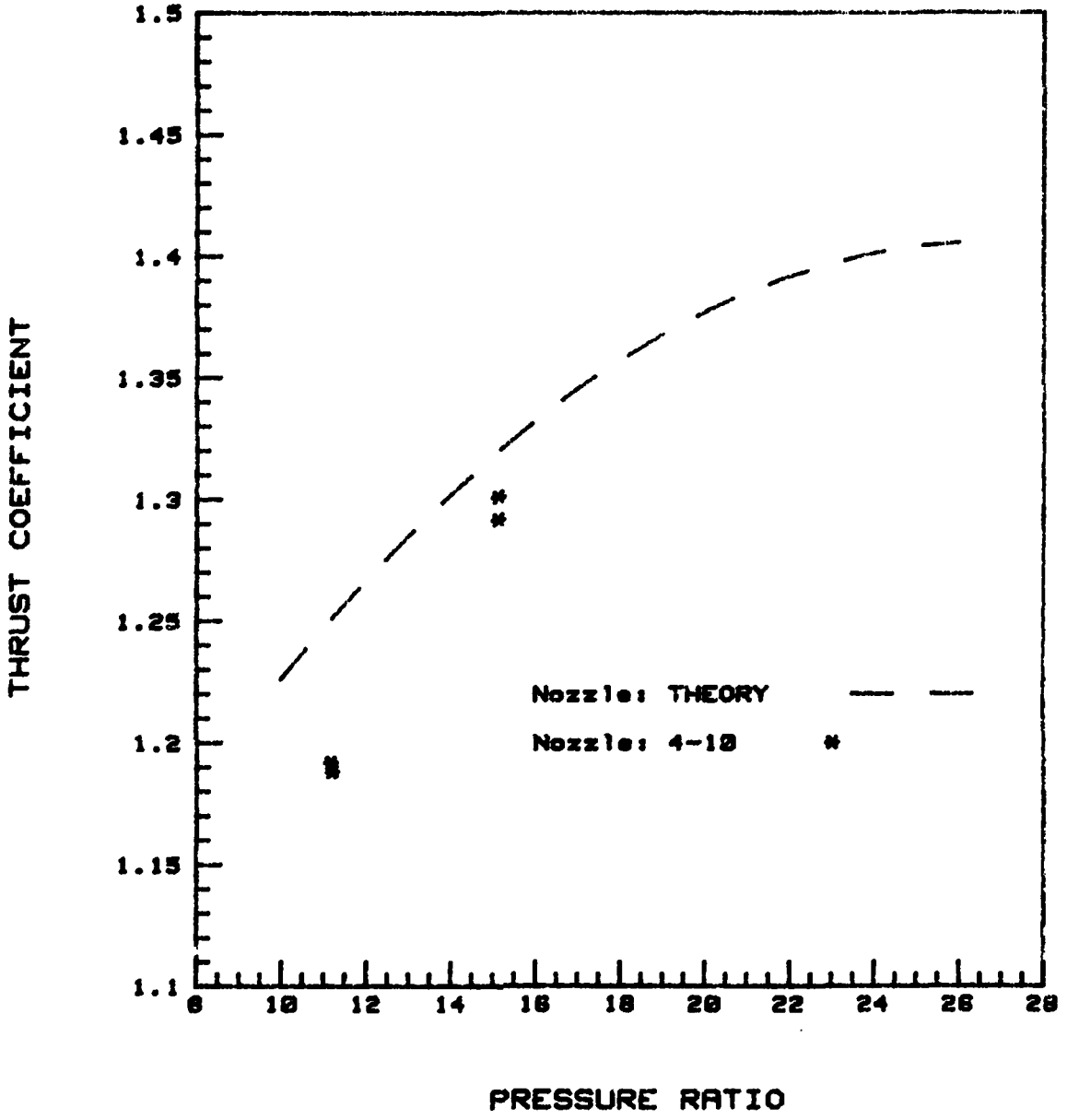

FIG A-17. Performance Comparsion of Nozzle 4-10 with Theory.

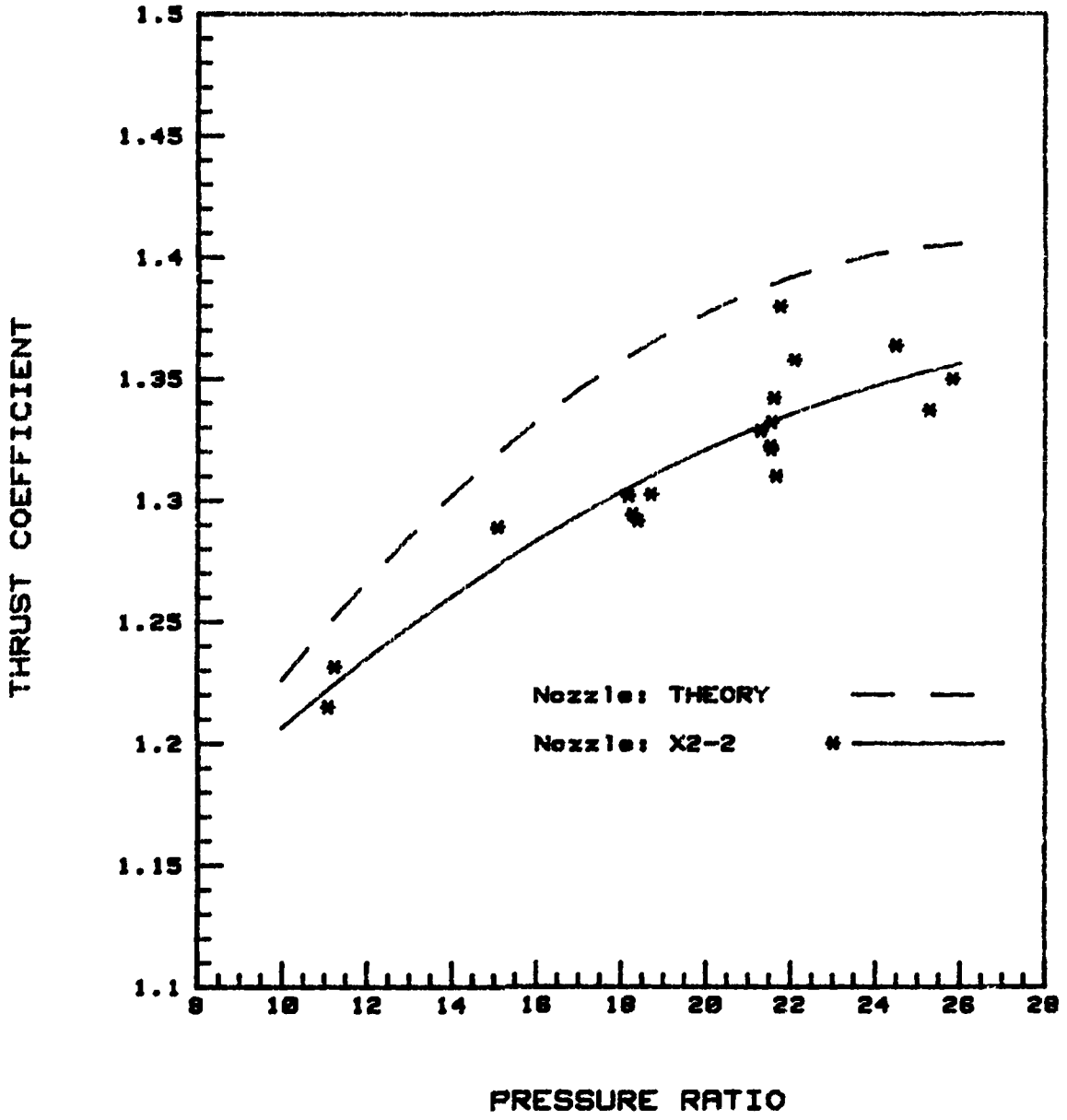

FIG A-16. Performance Comparsion of Nozzle X2-2 with Theory.

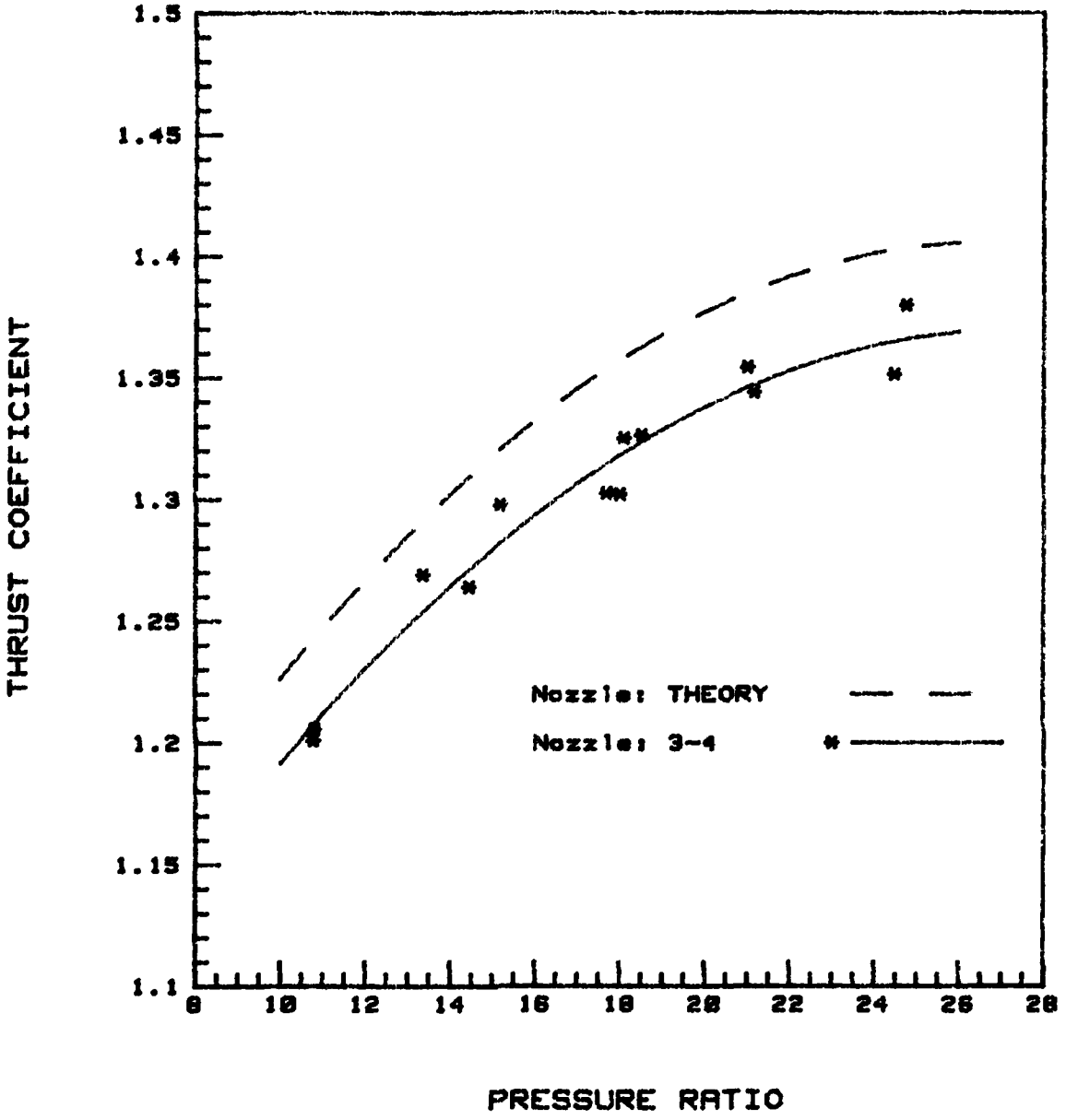

FIG A-18. Performance Comparsion of Nozzle 3-4 with Theory.

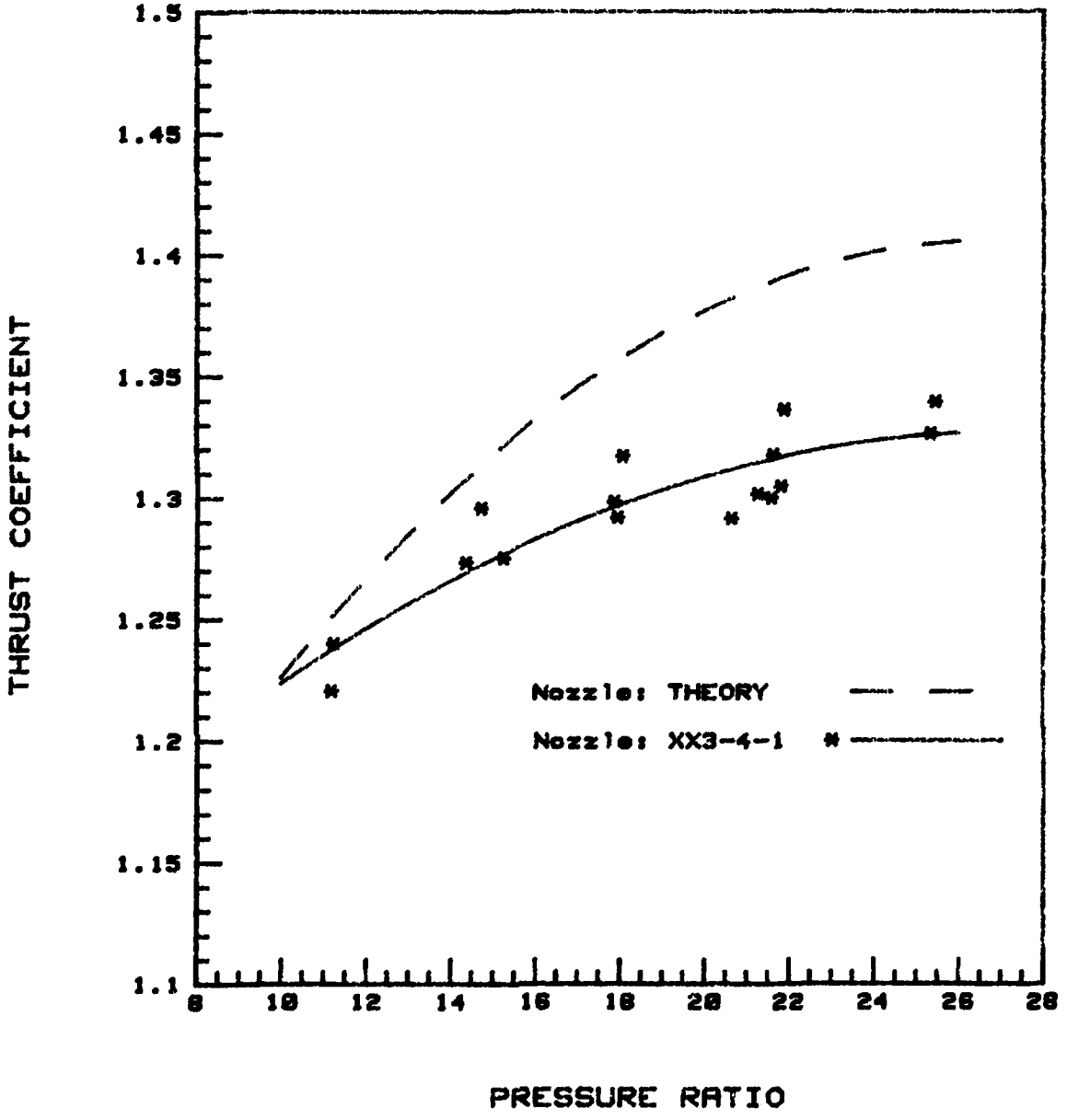

FIG A-20. Performance Comparsion of Nozzle XX3-4-1 with Theory.

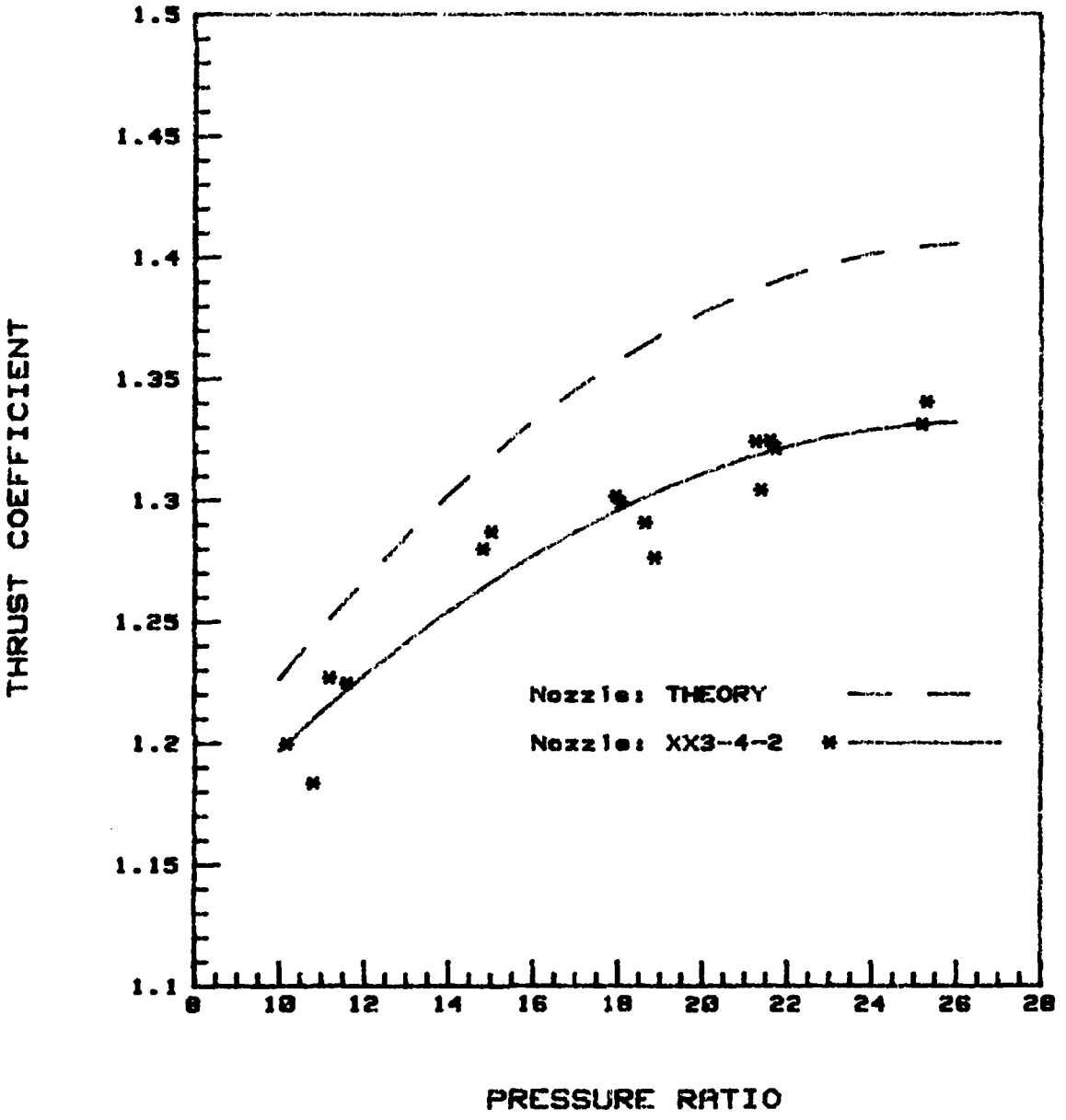

FIG A-21. Performance Comparison of Nozzle XX3-4-2 with Theory.

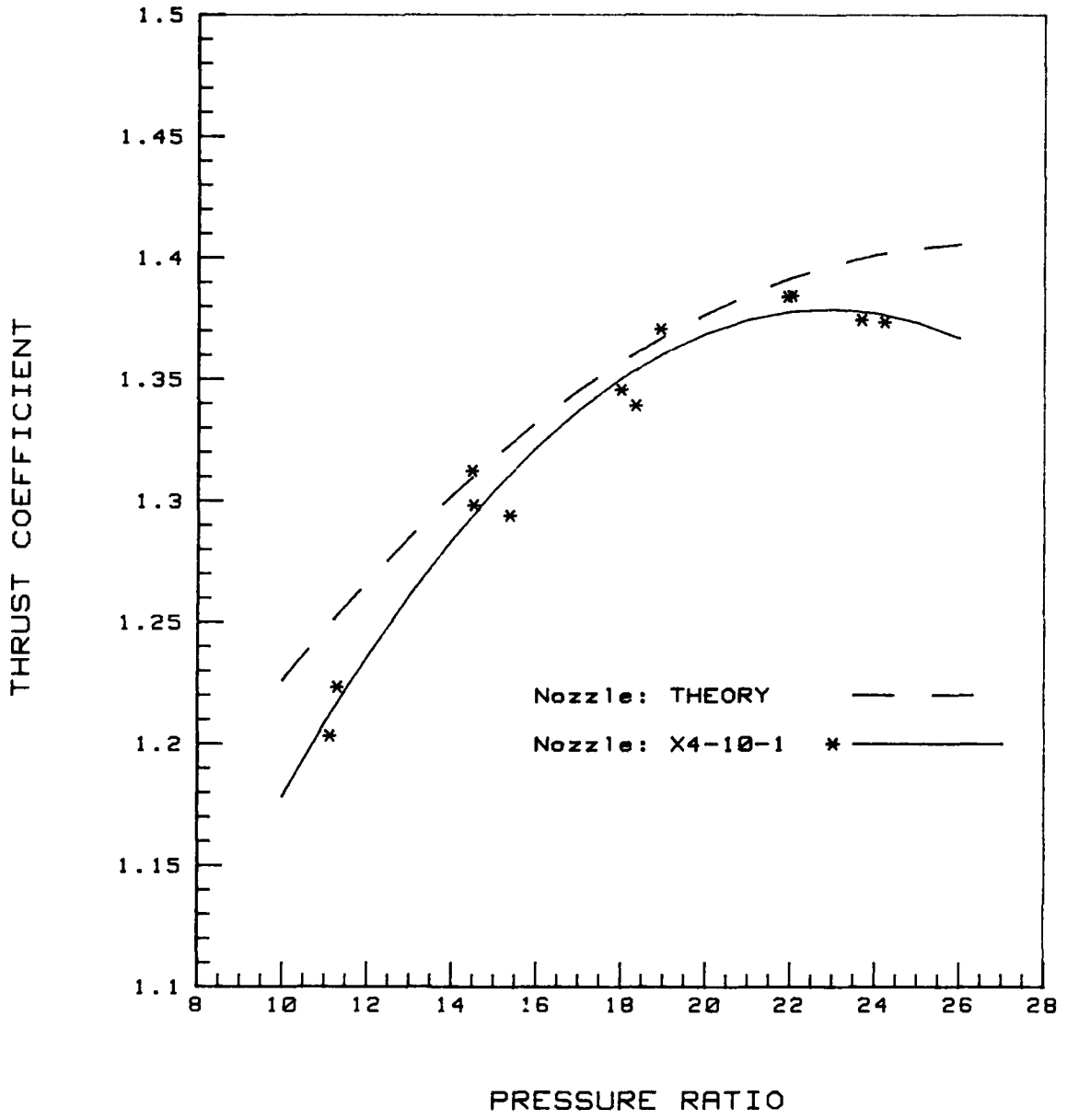

FIG A-22. Performance Comparsion of
Nozzle X4-10-1 with Theory.

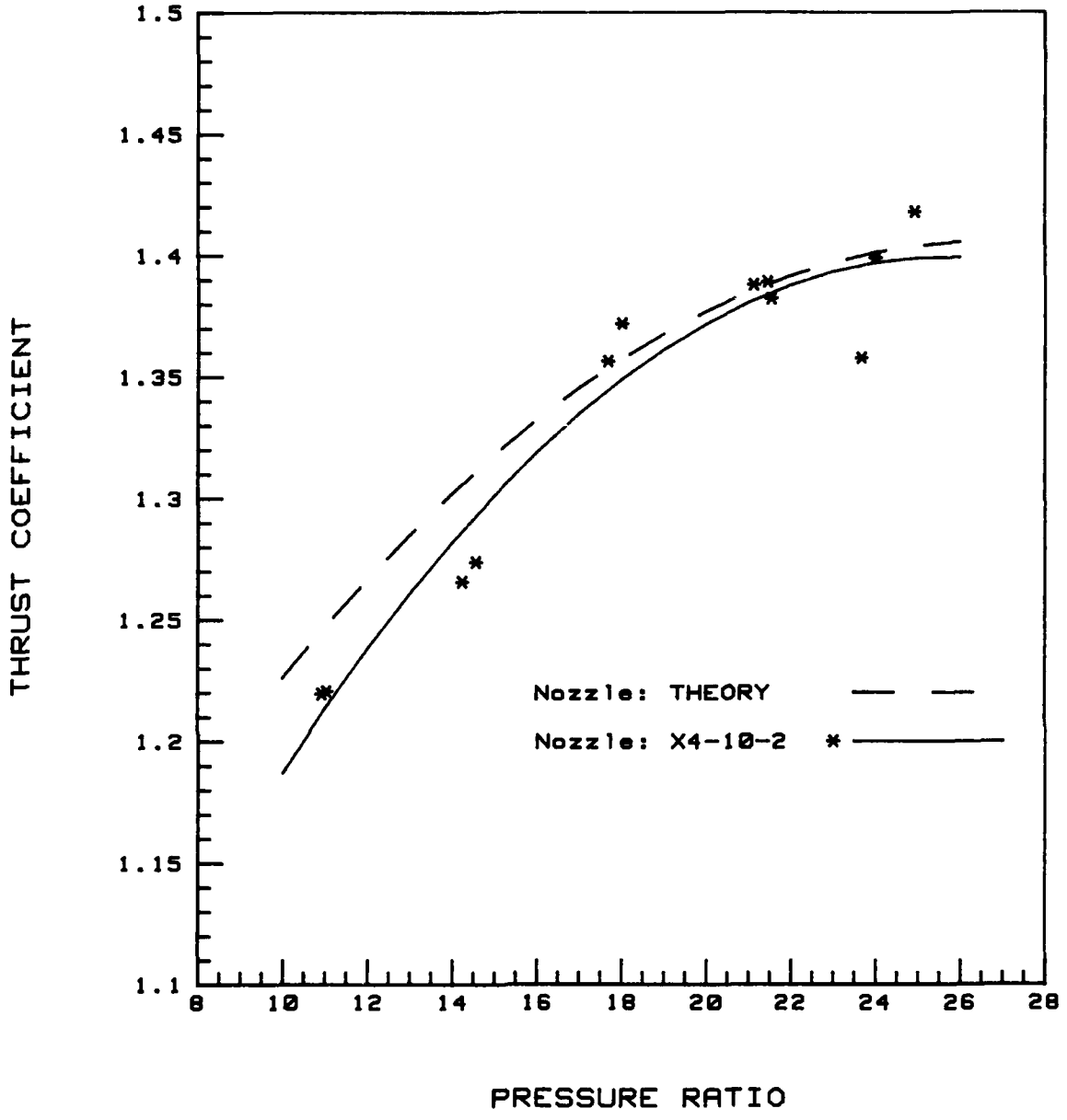

FIG A-23. Performance Comparsion of Nozzle X4-10-2 with Theory.

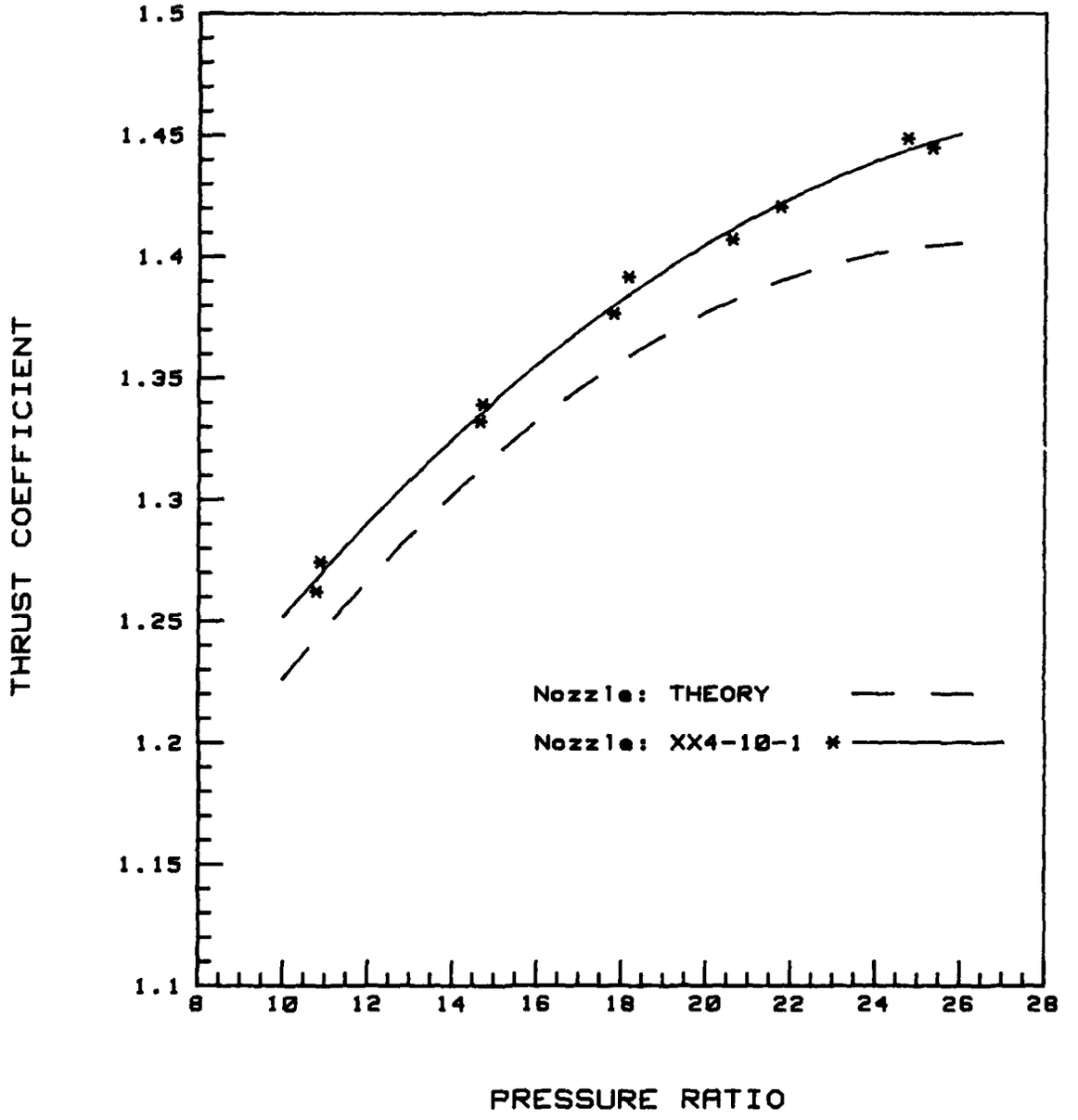

FIG A-24. Performance Comparsion of
Nozzle XX4-10-1 with Theory.

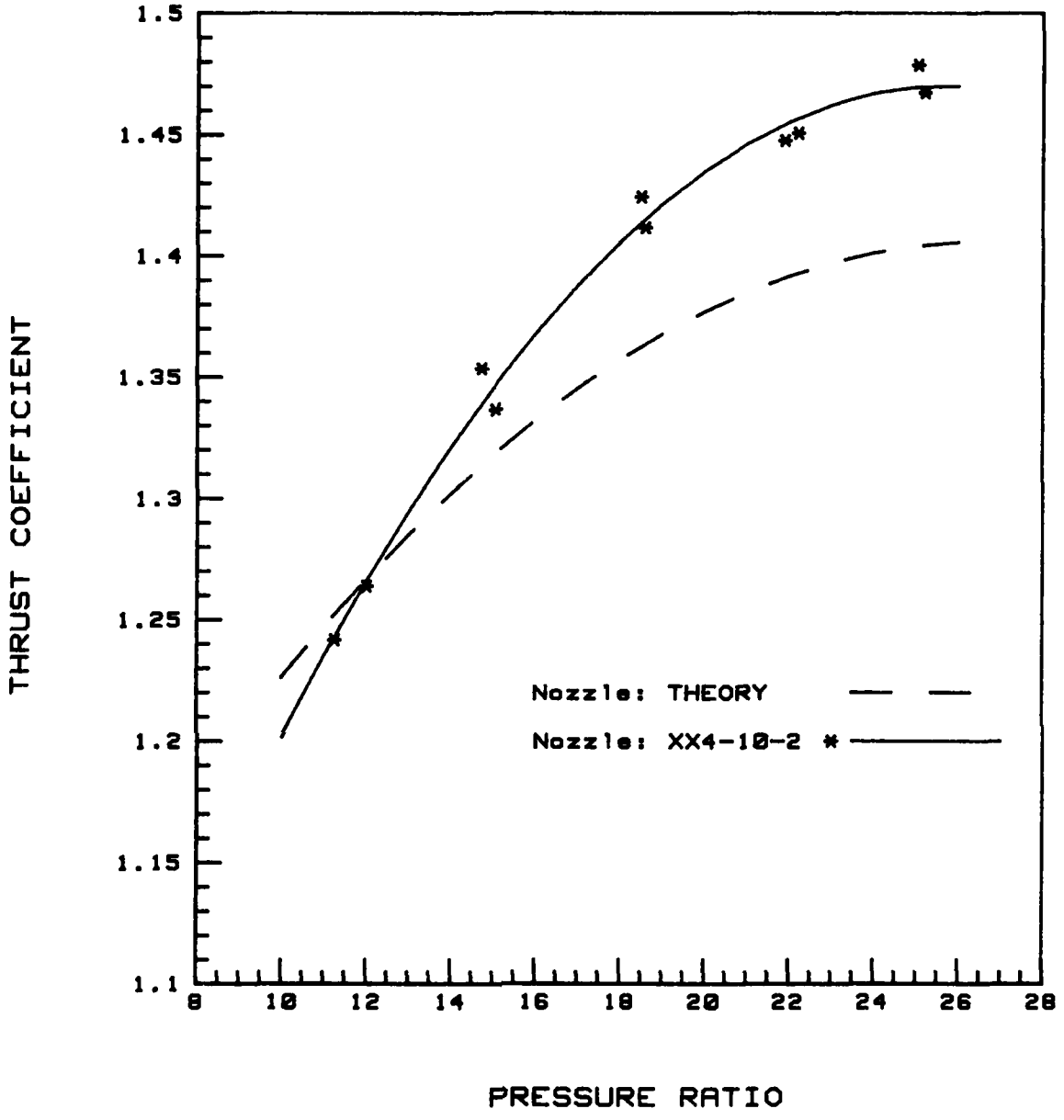

FIG A-25. Performance Comparsion of Nozzle XX4-10-2 with Theory.

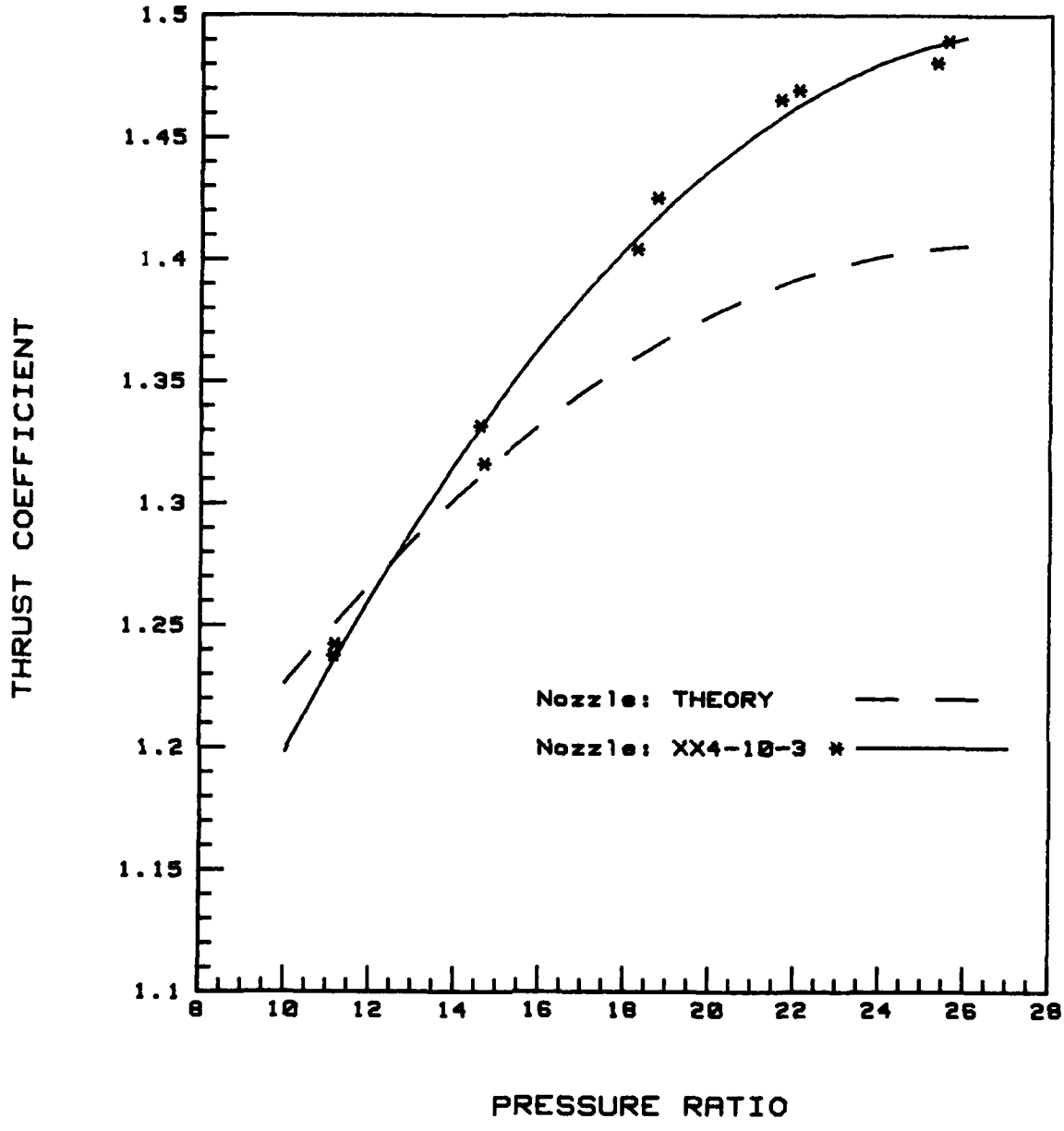

FIG A-26. Performance Comparsion of Nozzle XX4-10-3 with Theory.

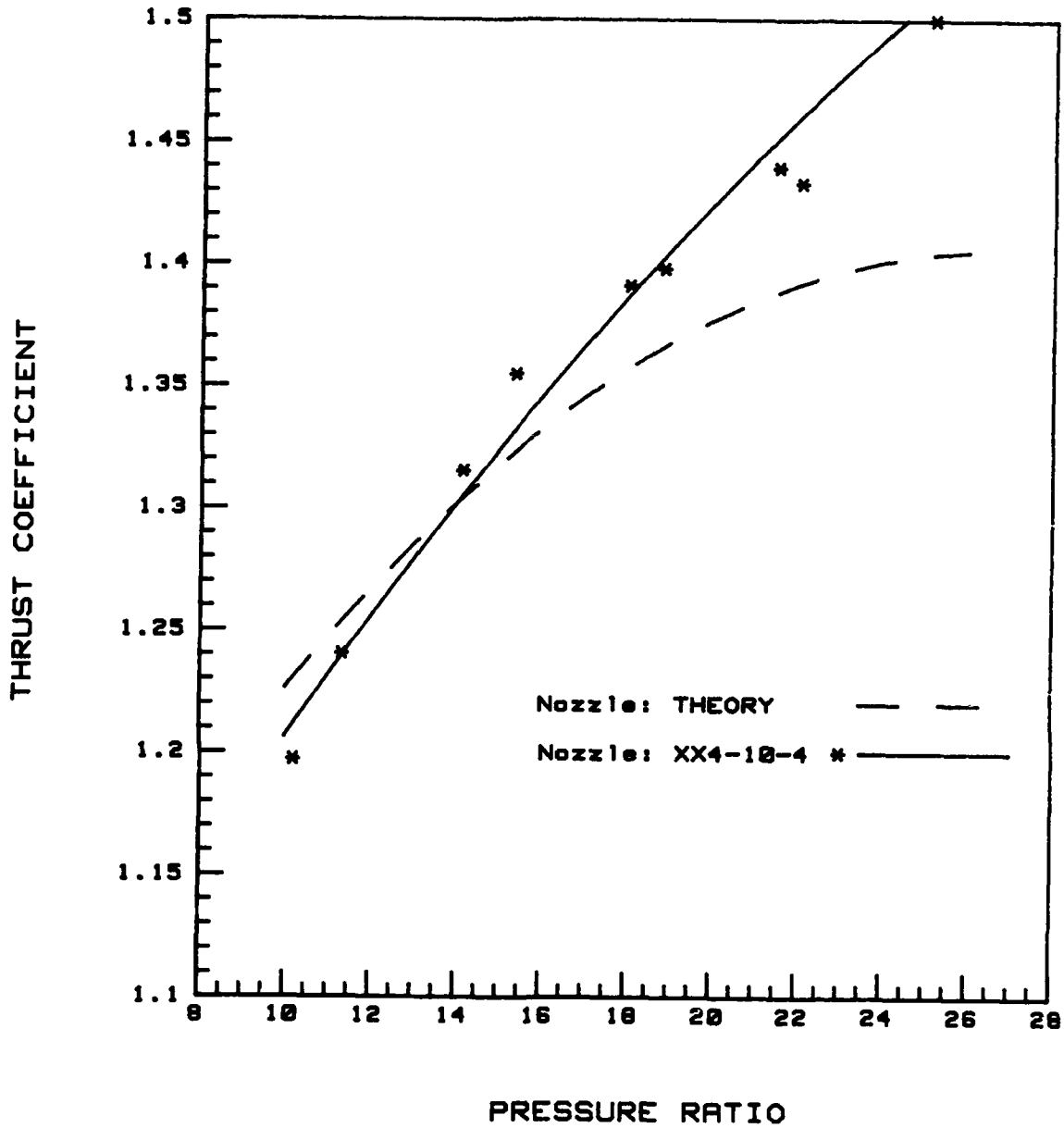

FIG A-27. Performance Comparsion of Nozzle XX4-10-4 with Theory.

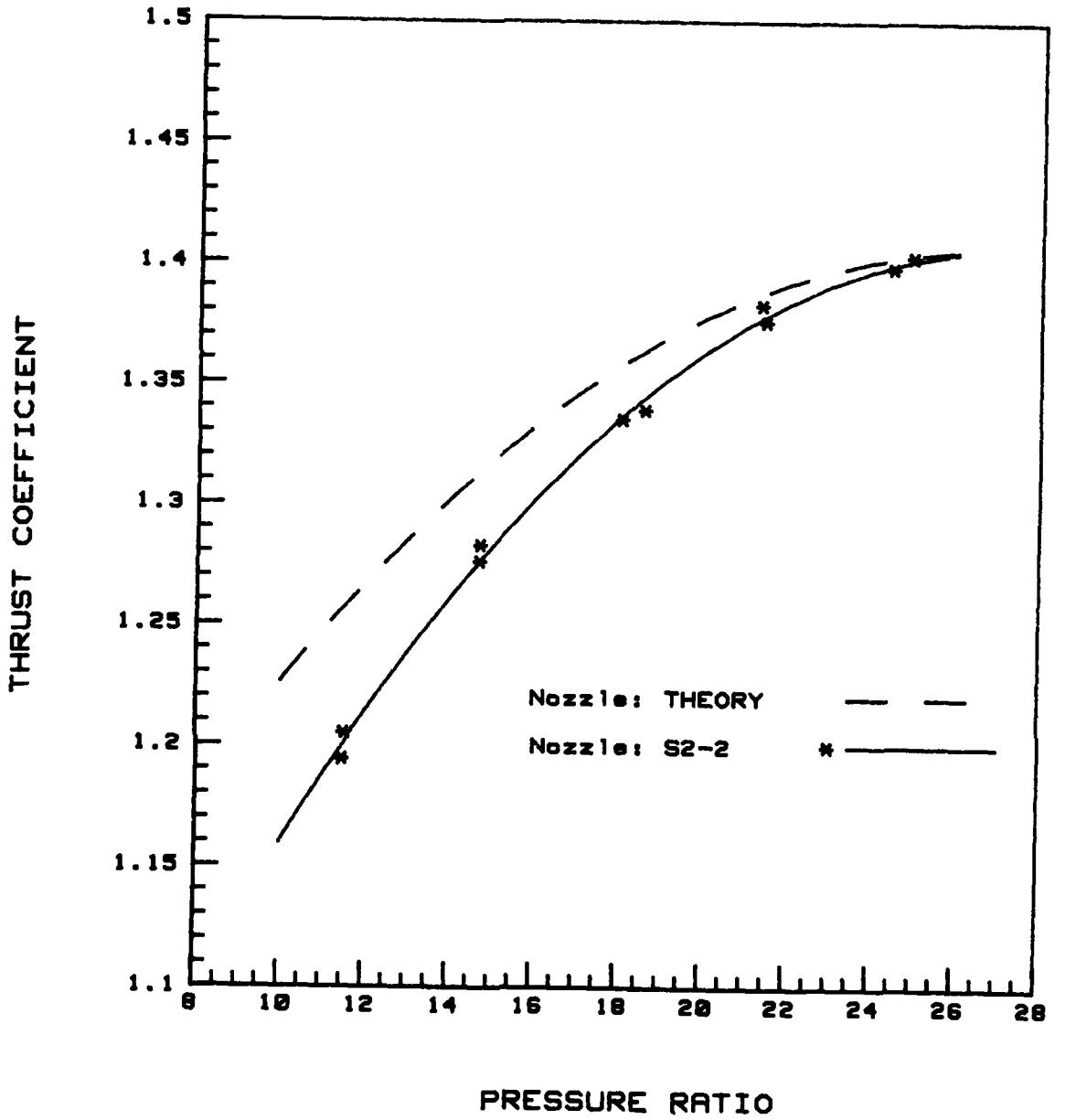

FIG A-28. Performance Comparsion of Nozzle S2-2 with Theory.

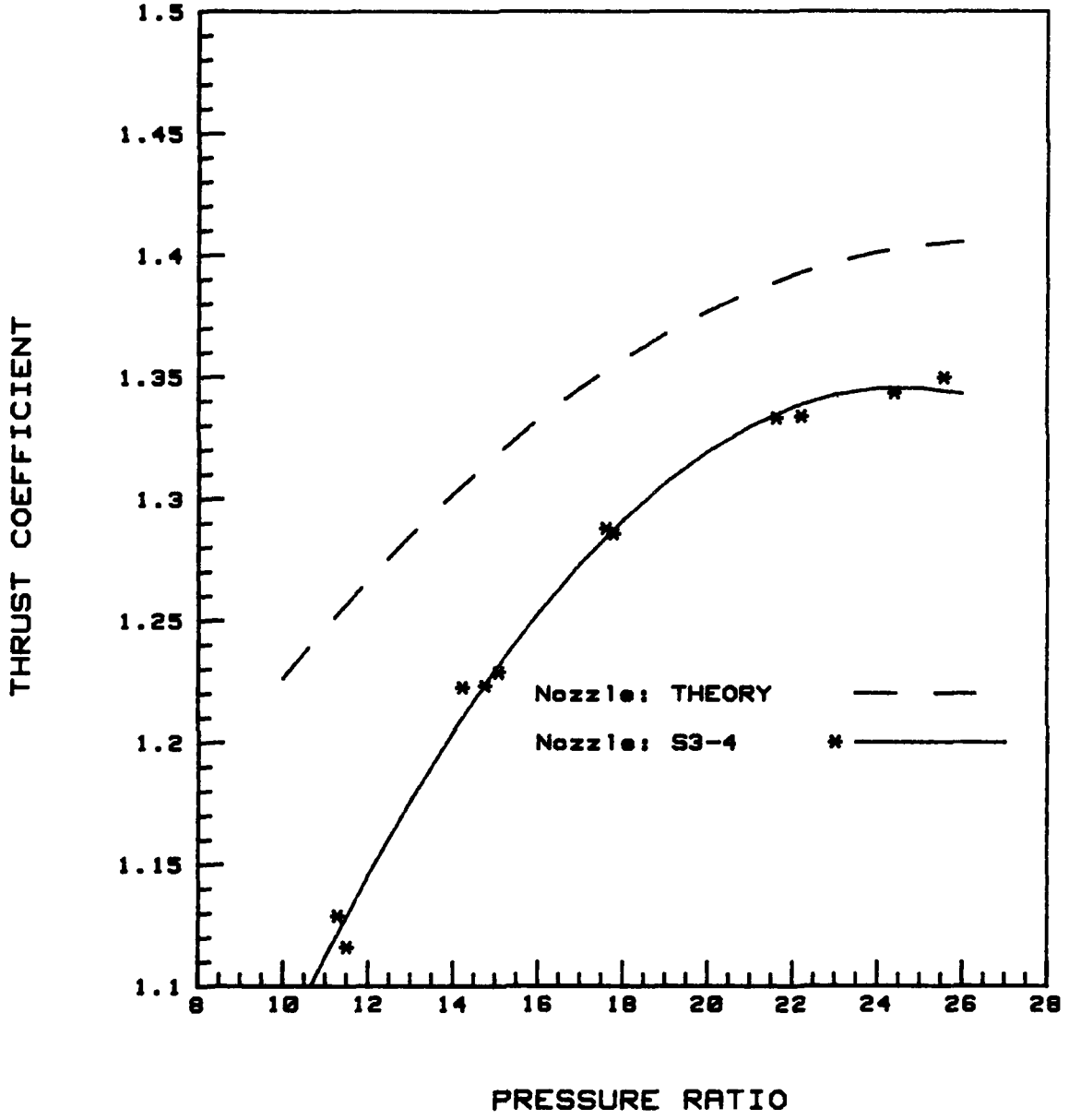

FIG A-29. Performance Comparsion of Nozzle S3-4 with Theory.

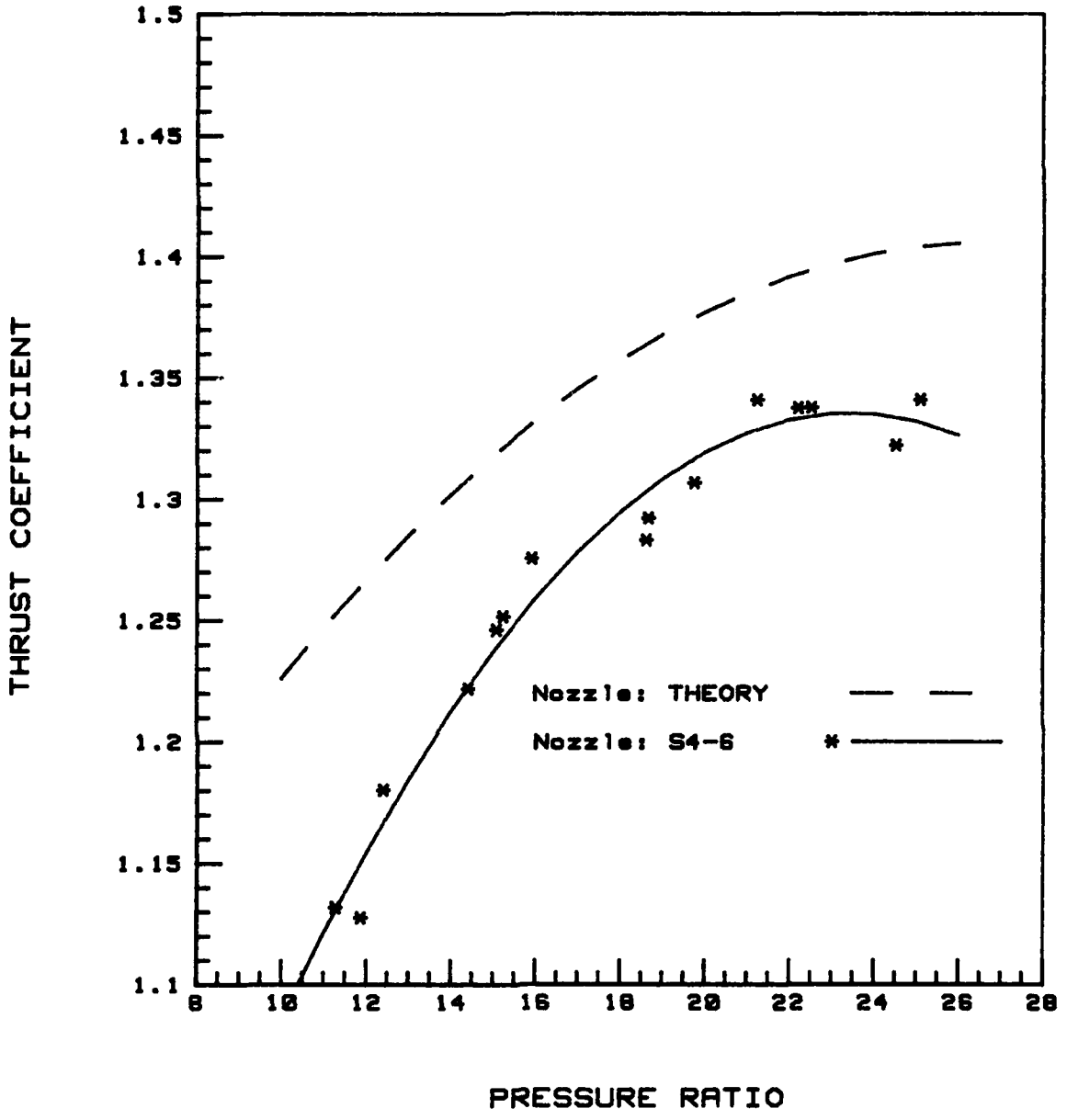

FIG A-30. Performance Comparsion of Nozzle S4-6 with Theory.

Appendix B

Figure B-1. Pendulum Structure with Stilling Chamber

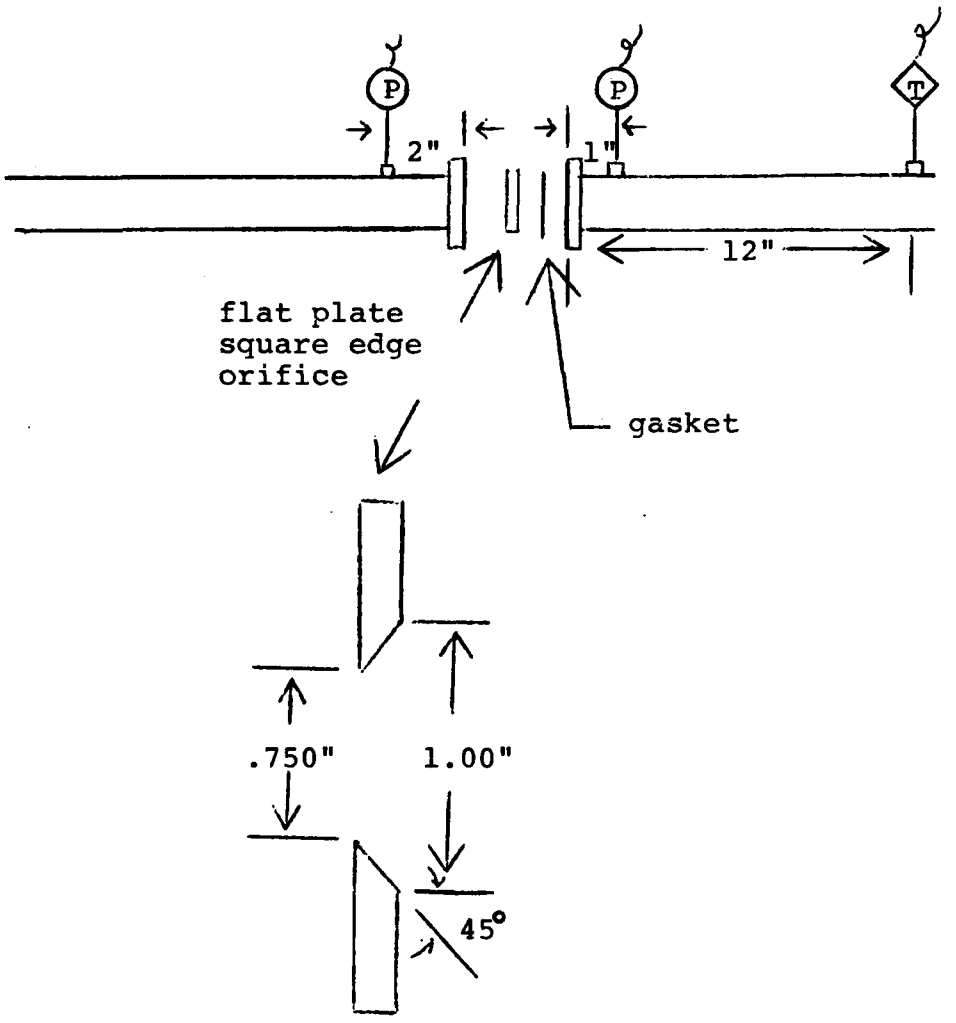

All dimensions in inches

P - pressure transducer
T - thermocouple

Figure B-2. Mass Flow Meter

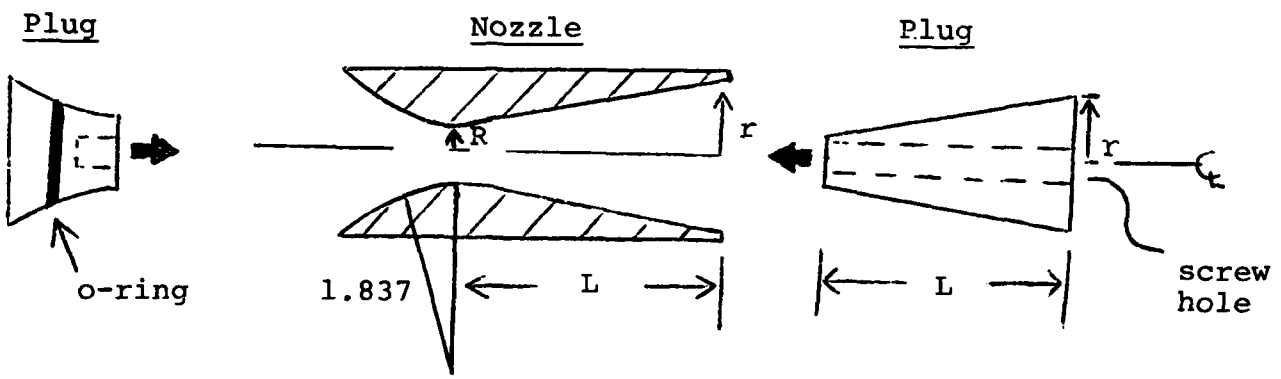

All dimensions in inches

Nozzle	R	A_t	r	L
1	0.307	0.2945	0.5303	2.241
2	0.222	0.1472	0.3749	1.584
3	0.153	0.0736	0.2650	1.119
4	0.127	0.0491	0.2165	0.915

Figure B-3. Nozzle and Plug Design

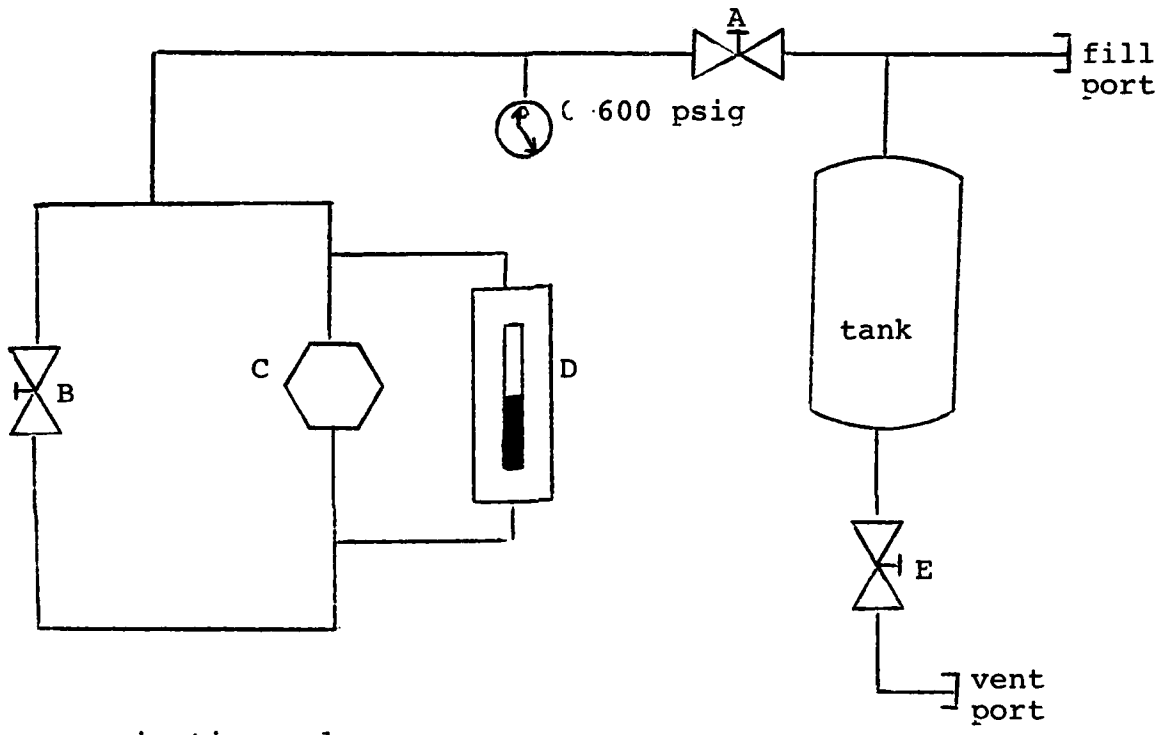

where

A - pressurization valve

B - pressure difference control valve

C - PSID pressure transducer (being calibrated)

D - manometer (Hg)

E - vent valve

Figure B-4. PSID Transducer Calibration System

Appendix C

Mass Flow Calculations

A thrust value can be calculated using the mass flow through the nozzle and nozzle flow theory. This calculated thrust may then be compared to the measured thrust. For the single nozzles, this provided a way of verifying the thrust measurement. Unfortunately, the calculated thrust will not reflect any potential thrust change due to clustering or inoperable nozzles because these effects are due to events outside the nozzle and will not effect the mass flow.

Mass Flow Calculation Methods

The mass flow can be calculated from measured data in two ways. Method I uses an orifice flow meter and is based on the pressure drop across the orifice. Method II uses the tank pressure and temperature along with isentropic flow theory to expand the gas out the nozzle.

Method I - Orifice Flow Meter. Reference 1 gives the following equation for calculating the mass flow from an orifice meter:

$$\dot{m} = \pi/4(d)^2 K \quad 2g_c\rho(\Delta p) \qquad \text{(C-1)}$$

where

$\dot{m}$ = mass flow (lbm/sec)
d = orifice diameter
= .75 in
K = flow constant
g_c = gravity constant
= 32.2 (lbm · f)/(lb_f · S^2)
ρ = density (lbm/ft^3)
Δp = pressure drop across orifice (psi)

The equation of state gives:

$$\rho = P_a/(R_c t_a Z) \qquad \text{(C-2)}$$

where

P_a = pressure prior to orifice (psia)
R_c = gas constant for air
= 53.35 (lb_f ft)/(R lbm)
t_a = air temperature
Z = compressibility factor
= .99 for 150-350 psia

Substituting equation (C-1) into equation (C-2):

$$\dot{m} = \pi/4d^2 \, K \sqrt{\frac{2g_c}{R}} \sqrt{\frac{P_a(\Delta p)}{t_a}} \qquad \text{(C-3)}$$

combining constants

$$\dot{m} = C_1 \sqrt{\frac{P_a(\Delta p)}{t_a}} \qquad \text{(C-4)}$$

Since K is a function of the flow conditions, therefore, C_1 is a function of the flow conditions. The K value is taken from a K versus Reynolds Number (Re) plot (Ref. 1:147). Each mass flow value has a corresponding Reynolds Number, and since K is constant for a range of Reynolds Number, a value of K can be selected for a range of mass flow. Table C-I provides the values of K for a given range of the corresponding values of the constant, C_1.

Table C-I Values of C_1 (Mass Flow Constant)

$\dot{m}$ lbm/sec	Re	K	C_1
.1→ .3	1.7×10^5→ 5.1×10^5	.6005	.2913
.3→ .8	5.1×10^5→ 1.4×10^6	.5967	.2895
.8→	1.4×10^6→	.5958	.2891

With the constants given in Table C-I and the pressure and temperature data at the orifice, a mass flow can be calculated using equation (C-4).

Method II. Isentropic Flow. The principal of continuity gives at the throat:

$$\dot{m} = \rho_t A_t V_t \qquad \text{(C-5)}$$

where

$$\rho_t = p_t / R_c t_t$$
$$V_t = M_t A_t$$

where: M_t = mach number
= 1.0 at the throat
A_t = speed of sound at throat
= $\sqrt{g_c \gamma R t_t}$ (γ = 1.4)

Isentropic flow tables (Ref. 6) gives at M = 1.0;

$$P_t = .52828\ P_o$$
$$t_t = .8333\ t_o$$

where

P_o = chamber pressure (psia)
t_o = chamber temperature (R)

Substituting constants:

$$\dot{m} = .522\ (P_o\ A_t\ \sqrt{t_o})\ \text{lbm/s} \qquad \text{(C-6)}$$

Therefore, if the chamber conditions are known, the mass flow can be calculated.

Method I was used for configurations that had a mass flow of over .5 lbm/s, which included the two large single nozzles, all fully flowing clusters (both shrouded and unshrouded) and most of the clusters with inoperable nozzles. The second method (Method II) was used as a back-up for the first method and was the primary method for the smaller nozzle configurations due to extremely low pressure differentials across orifice.

Thrust Calculations

Once the mass flow was calculated, the basic thrust equation (equation (1) in the main text) was used to calculate the thrust. The equation is given again below.

$$T_c = mV_e + (P_e - P_3)\, A_e \qquad \text{(C-7)}$$

where

T_c = calculated thrust

The isentropic flow tables allows us to write the equation in terms of the stilling chamber parameters. The flow tables (Ref. 6) provides the following relationships for a nozzle exit area ratio of 3.0:

$$M_e = 2.63$$
$$t_e = .4198\ t_o$$
$$P_e = .0478\ P_o$$

Combining the constants, the thrust equation becomes:

$$T_c = 2.60\ \dot{m}\ \sqrt{t_o} + (.0478\ P_o - P_3)\, A_e \qquad \text{(C-8)}$$

All the parameters on the right side of equation (C-8) are measured or known, and, therefore, the thrust can be calculated. Finally, for comparison purposes, the thrust coefficient is determined by:

$$Cf_c = T_c/P_o\, A_t \qquad \text{(C-9)}$$

Comparison of Calculated and Measured Thrust

Table C-II compares the calculated thrust coefficient to the measured thrust coefficient for several nozzle configurations. The values are given for the optimum expansion condition.

Table C-II Thrust Coefficient Comparison
(Calculated vs Measured)

Nozzle	C_{f_m}	C_{f_c}	Δ%
01	1.38	1.32	4.3
02	1.37	1.40	-2.2
03	1.37	1.38*	-0.7
04	1.37	1.38*	0
2-2	1.38	1.32	4.3
3-4	1.38	1.32	4.3
4-6	1.34	1.31	2.6
XX3-4-2	1.32	1.35	-2.3
X4-10-1	1.38	1.37	0.7
XX4-10-3	1.47	1.39*	5.4
S3-4	1.33	1.29	3.0

*C_{f_c} Calculated using Method II.

$$\Delta\% = \frac{C_{f_m} - C_{f_c}}{C_{f_m}}$$

Vita

James T. Lester, Jr., was born February 1, 1956, in Washington D.C. In 1974, he graduated from Hamilton Township High School, Columbus, Ohio. He attended Ohio State University from September 1974 to June 1978 and received a B.S.A.A.E. degree. He was commissioned in the United States Air Force through the R.O.T.C. program in June 1978. His initial assignment was at the Air Force Rocket Propulsion Laboratory, Edwards A.F.B., California. He worked as a Satellite Engine Test Engineer from August 1978 to May 1981. He entered A.F.I.T. in June 1981.

Permanent Address: P. O. Box 97
Stevinson, California 95374

UNCLASSIFIED
SECURITY CLASSIFICATION OF THIS PAGE *(When Data Entered)*

REPORT DOCUMENTATION PAGE		READ INSTRUCTIONS BEFORE COMPLETING FORM
1. REPORT NUMBER AFIT/GAE/AA/82D-18	2. GOVT ACCESSION NO. AD-A124 677	3. RECIPIENT'S CATALOG NUMBER
4. TITLE *(and Subtitle)* AN EXPERIMENTAL STUDY OF CLUSTER NOZZLE PERFORMANCE		5. TYPE OF REPORT & PERIOD COVERED MS Thesis 6. PERFORMING ORG. REPORT NUMBER
7. AUTHOR(s) James T. Lester Jr. Capt		8. CONTRACT OR GRANT NUMBER(s)
9. PERFORMING ORGANIZATION NAME AND ADDRESS Air Force Institute of Technology (AFIT/EN) Wright-Patterson AFB, Ohio 45433		10. PROGRAM ELEMENT, PROJECT, TASK AREA & WORK UNIT NUMBERS
11. CONTROLLING OFFICE NAME AND ADDRESS Air Force Rocket Propulsion Laboratory (AFRPL) Edwards AFB, Ca 93523		12. REPORT DATE December 1982 13. NUMBER OF PAGES 79
14. MONITORING AGENCY NAME & ADDRESS*(if different from Controlling Office)*		15. SECURITY CLASS. *(of this report)* Unclassified 15a. DECLASSIFICATION/DOWNGRADING SCHEDULE

16. DISTRIBUTION STATEMENT *(of this Report)*

Approved for public release; distribution unlimited

17. DISTRIBUTION STATEMENT *(of the abstract entered in Block 20, if different from Report)*

18. SUPPLEMENTARY NOTES

Approved for public release: IAW AF
LYNN E. WOLAVER
Dean for Research and Professional Development
Air Force Institute of Technology (ATC)
Wright-Patterson AFB OH 45433

16 JAN 1983

19. KEY WORDS *(Continue on reverse side if necessary and identify by block number)*

Clustered Nozzles
Aerodynamic Shrouding
Supersonic Nozzles
Thrust Performance
Sealed Nozzles

20. ABSTRACT *(Continue on reverse side if necessary and identify by block number)*

Clusters of up to ten converging-diverging supersonic nozzles were cold flow tested at ambient conditions to determine their thrust performance as compared to a single nozzle of same total throat area. The nozzles were operated at both underexpanded and overexpanded conditions, and no significant thrust difference was detected between the clusters and single nozzles. Schlieren photograghs verified no interference between jets of different nozzles. Clusters with various patterns of flowing and non-

DD FORM 1 JAN 73 1473 EDITION OF 1 NOV 65 IS OBSOLETE

UNCLASSIFIED
SECURITY CLASSIFICATION OF THIS PAGE *(When Data Entered)*

flowing nozzles were also tested. The non-flowing nozzles had no effect on the flowing nozzles except when, due to the sealed nozzles, the base plate area was greatly increased. The increased base plate area resulted in a noticeable improvement of thrust over theoretical throughout the pressure ratio range tested with the greatest increase in the underexpanded region. The location or patterns of non-flowing nozzles were of no consequence. Finally, aerodynamic shrouding, with no spacing between the shrouding and the nozzle, was placed on the clusters and tested. There was a very slight decrease in thrust performance associated with a decrease in the base plate area.

END